약학박사학위논문

The Biophysical and Physiological Properties of TMEM150C and TMEM16H

TMEM150C와 TMEM16H의 채널특성과 생리적기능 연구

2020년 8월

서울대학교 대학원

약학과 병태생리학 전공

루후안준

ABSTRACT

TMEM150C, also known as TTN3, is a cation channel which can be stimulated by mechanical stimulation. The inactivation of TTN3 is a slow adaptation (SA) MA type compared to the rapid inactivation mechanics of Piezo1 or Piezo2. It has previously been reported that TTN3 is expressed in muscle spindle afferents and mediates muscle coordination. Since TTN3 is a MA channel, I hypothesized that TTN3 may be involved in detecting blood pressure changes in baroreceptor. Here I show that TTN3 is expressed in the nerve endings of aortic arch and nodose ganglia (NG) neurons. *Ttn3* KO promotes peripheral hypertension, tachycardia, large fluctuations in blood pressure, and impaired baroreceptor function. Chemogenetic silencing or stimulation of *Ttn3* positive neurons in NG can cause an increase or decrease in blood pressure and heart rate, respectively. More importantly, overexpression of *Ttn3* in *Ttn3*-/- mouse NG rescued cardiovascular changes in Ttn3-/- mice. My conclusion is that TTN3 is a molecular component that contributing to sensing the

dynamic changes of blood pressure in baroreceptors.

TMEM16, also known as Anoctamin (ANO) gene family consists of ten isoforms. ANO1 and ANO2 are recognized as anion channels activated by Ca2+. ANO6 is a scramblase that destroys polarized phospholipids in the membrane. However, the function of TMEM16H (ANO8) is still unknown. Here I found that ANO8 is a cation channel activated by intracellular cAMP. Inward currents in ANO8 overexpressing HEK cells were observed when intracellular cAMP. The cAMP dependent currents were inhibited by a protein kinase-A inhibitor, which indicates that protein kinase A plays an active role in its activation mechanism. Cholera toxin, an activating agent of adenylate cyclase also activated ANO8. The currents in ANO8 expression cells induced by cAMP were cationic because they did not discriminate among cations. ANO8 is highly expressed in neurons in the brain regions as well as dorsal root ganglion (DRG) neurons. Knock down of Ano8 causes a decrease in cAMP dependent currents in DRG neurons as well as nociceptive behaviors in the formalin pain mice model. These

results now suggest that ANO8 is a cation channel activated by the cAMP/pathway and involved in nociception in the pain pathway.

Student Number: 2015-30875

Keywords: TMEM150C/TTN3, TMEM16H/ANO8, ion channel, baroreceptor, nociception, cAMP/PKA, pain

TABLE OF CONTENTS

LIST OF FIGURES

INTRODUCTION

1. Ion channels

1.1. Overview

Ion channels are pore-forming proteins located in the plasma membrane. They are the pathways for the transport of various ions across the plasma membrane. Cells continue to carry out metabolic activities, they must constantly exchange substances with the surrounding environment, and the ion channel on the cell membrane is an important way to exchange this substance. Thus, Ion channels play wide-ranging physiological roles.

Ions flow passively through channels toward electrochemical equilibrium. The difference in electrical (voltage) or chemical (concentration) gradients can force the ions to move in or out of the cell. Thus, ion channels have played an important role in cell secretion and electrical signaling to adapting the environmental changes(Strickland et al., 2019) (Figure 1).

In addition, when the channels are in open state, the charged ions flow through the channels and represents an electrical current which changes the voltage across the membrane by altering the distribution of charge. In excitable cells, The transient influx of positive ions such as sodium and calcium ions go through voltage-gated channels to cause brief depolarizations of the membrane known as action potentials. Action potentials can be transmitted quickly over long distances, allowing for coordination and precise timing. In almost all cases, the action potential triggers downstream physiological effects, such as secretion or muscle contraction, by opening voltage-gated calcium-selective ion channels and increasing intracellular calcium concentration(Catterall, 2011).

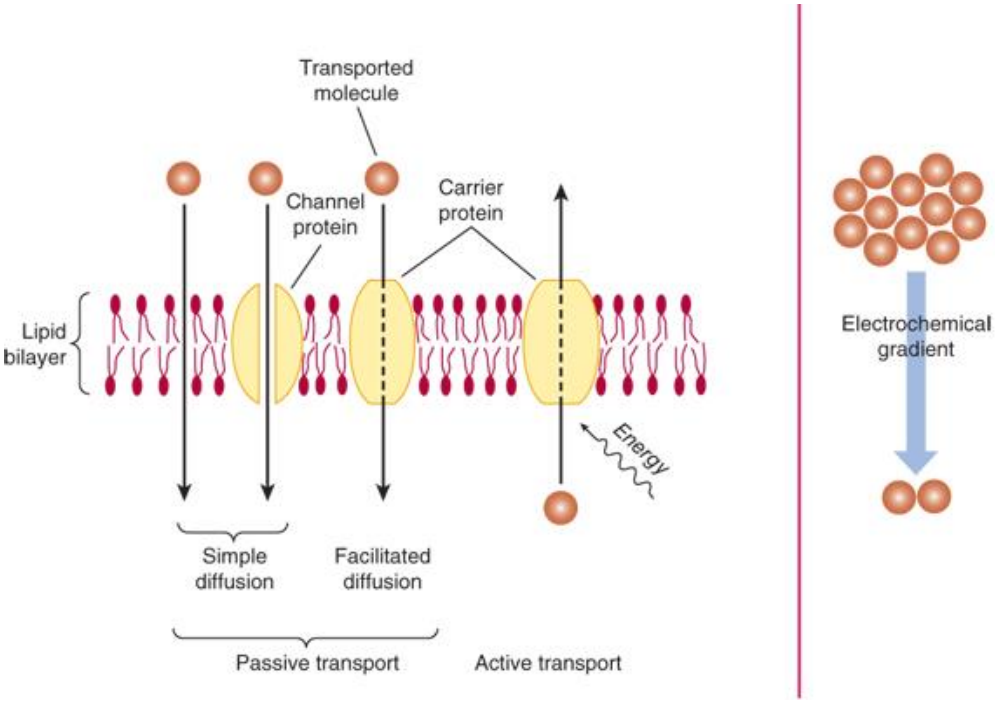

Figure 1. Ion transport through ion channel

Ions pass through channels down their electrochemical gradient, which is a function of ion concentration and membrane potential, without the input (or help) of metabolic energy (such as ATP, co-transport mechanisms, or active transport mechanisms. Reference from (Rodwell et al, 2018)

1.2. Classification of ion channels

According to the properties of conducting ions, Ion channels can be divided into two broad groups: anion and cation channels. Most of anion channels conduct Cl^- and can be divided into ClC family (Jentsch et al., 1990), Cystic fibrosis transmembrane conductance regulator (CFTR) (Wine et al., 1991), Calcium-activated chloride channel (CaCC) (Kuruma and Hartzell, 1999), Maxi chloride channel (Christensen and Zeuthen, 1987), and Volume regulated chloride channels (VRAC) (Worrell et al., 1989). According to the different ion selectivity or permeability, cationic channels can be divided into five groups: potassium channels, proton channels, Ca^{2+} channels, Na^+ channels and non-selective cation channels.

Ion channels can also be classified according to how the chemical or physical stimulator controls their gating mechanism. The most common groups of ion channels are voltage-gated ion channels such as voltage-gated potassium channels, voltage-gated calcium channels, voltage-gated sodium channels. These channels

can be activated by membrane potential change.

Some ion channels such as 5-HT3 serotonin receptor, ATP-gated P2X receptors and GABA-A receptor, whose gating mechanism is binding a ligand. So, these kinds of ion channels were classified as ligand-gated ion channels, also known as ionotropic receptors. When some kind neurotransmitter binds to the extracellular membrane region, it will cause the cell membrane structural change. This membrane structural change can make the channel become open state. Transient receptor potential TRP channels are activated by chemicals, Ca2+ and temperature change(Zheng, 2013). The send messenger inside of the cell such as Ca2+, cAMP or cGMP also can affect the gating mechanism such as Ano1 and Ano2 can be activated by intracellular calcium(Jin et al., 2016). Cyclic nucleotide-gated channels (CNG channel) are characterized by activation by either intracellular cAMP or cGMP(Biel, 2009). Mechanosensitive channels are the channels gated by osmotic shock, positive or negative pressure in plasma membrane.

1.3. TMEM16 (Anoctamin) Family

1.3.1. Overview

Calcium-activated chloride channels (CaCCs) are groups of ligand-gated chloride channels which open in response to a change in intracellular calcium concentration (Yang et al., 2008a). TMEM16A, the first member of the TMEM16 family, was cloned by three labs (Caputo et al., 2008; Schroeder et al., 2008; Yang et al., 2008a; Yang et al., 2008b), This family was named as anoctamin due to initial prediction of their eight-transmembrane domain structure. Anoctamins family contains ten genes in mammal, and Yang et al (Yang et al., 2008a) cloned TMEM16A. The anoctamin/TMEM16 family consists of 10 isoforms (Figure 2)(Duran and Hartzell, 2011). The activity of anoctamins was observed in variable tissues and different physiological functions of anoctamins were reported.

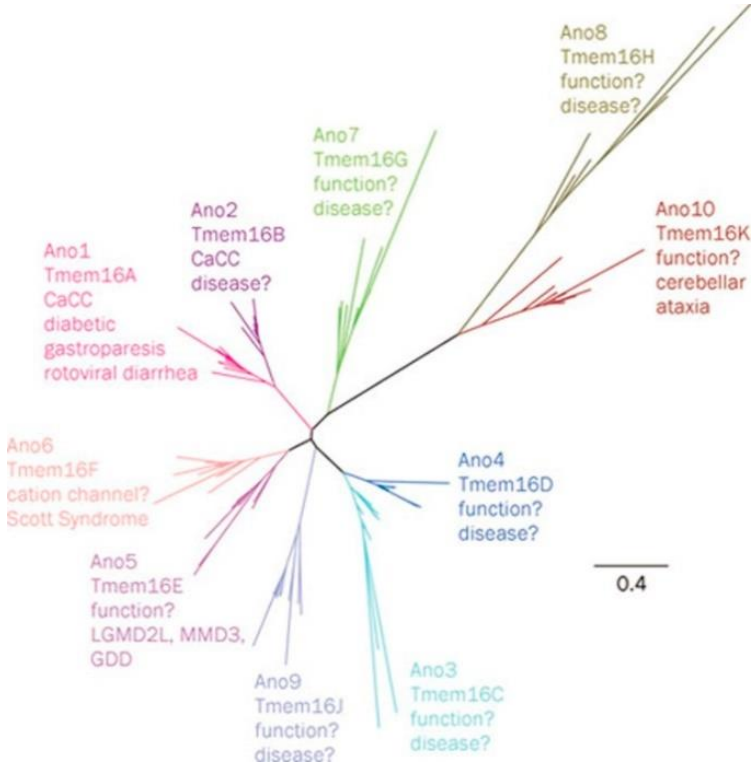

Figure 2. Phylogenetic tree and physiological functions of Anoctamins Reference from (Duran and Hartzell, 2011)

1.3.2. Physiological functions of anoctamins

1.3.2.1. Anoctamin 1 (ANO1)

Ano1, also called TMEM16A, is the most well-known member of anoctamins family(Yang et al., 2008a). Ano1 is a classical calcium activated chloride channel. When the concentration of intracellular Cl^- increase, Ano1 will be activated. Ano1 is widely expressed virous organs especially in secretory epithelia, for example, salivary gland(Catalan et al., 2015), pancreas(Xu et al., 2014), gut(Stanich et al., 2011), mammary gland, and airway epithelium(Huang et al., 2012a).

Ano1 is also found in various kinds of smooth muscle including vascular smooth muscle cells(Wang et al., 2016). Ano1 is strongly expressed in airway smooth muscle cells, suggesting the possibility that this channel might be involved in asthma. Ano1 originally attracted the interest of cancer biologists because it is overexpressed in many tumors(Carles et al., 2006; West et al., 2004). Ano1 may become a very useful tool for the diagnosis of different cancers. Ano1 is also expressed in small DRG neurons

and mediate with nociceptive stimuli as a heat sensor(Cho et al., 2012). In addition, ANO1 is expressed in the human gastrointestinal epithelium and in the gastrointestinal interstitial cells of Cajal, where it may participate in epithelial chloride secretion(Malysz et al., 2017).

1.3.2.2. ANO2

Ano2 is one of the members of Anoctamin family and also identified as calcium activate chloride channel. Previous study already shows that in olfactory sensory neurons(Li et al., 2018). Ca2+ influx through the cyclic nucleotide gated channels then activates Ano2 that amplify the receptor potential. So Ano2 is now suggested to the best candidate for CaCCs in olfactory sensory neurons(Li et al., 2018). Ano2 is known to modulate the synaptic transmission between C3 region and CA1 region in the hippocampus and controls action potential firing frequency(Huang et al., 2012b). Ano2 is also well known to mediate spike-frequency adaptation in thalamocortical neurons(Ha et al., 2016). The

significantly reduced spike-frequency adaptation along with increased tonic spiking was found in thalamocortical neurons after knockdown of Ano2. Recent reports show that Ano2 is expressed in inferior olivary neurons that sends climbing fibers to innervate Purkinje cells for motor learning(Zhang et al., 2017).

1.3.2.3. ANO3

Whether Ano3 is an ion channel is not clear. ANO3 is well known to modulate Slack channel in a subset of DRG neurons(Huang et al., 2013). Slack expression in rat DRG neurons largely decreased when knockout of Ano3. Ano3 knock out rat as well as Slack knockdown rat showed increased thermal and mechanical sensitivity. Ano3 was suggested to improve K Na channel activity in DRG neurons and regulates the processing of pain.

1.3.2.4. ANO5

Mutations in Ano5 are associated with a spectrum of

musculoskeletal disorders. Ano5 was originally identified as GDD1, the gene product mutated in a rare autosomal dominant skeletal syndrome called gnathodiphyseal dysplasia (GDD)(Lv et al., 2019). Mutations in cysteine-356, a highly conserved cysteine in the first extracellular loop of Ano5, results in abnormal bone mineralization and bone fragility. Although some function of Ano5 still need to be discovered, it indeed plays important roles in musculoskeletal development. Also, Ano5 is found in growth-plate chondrocytes and osteoblasts for activing bone turnover, suggest that Ano5 may participate in bone formation(Silva et al., 2019). Although Ano5 appears to be related to bone formation, whether it is a channel or not is still unclear.

1.3.2.5. ANO6

Ano6/TMEM16F is a calcium dependent phospholipid scramblase. Mutations in Ano6 have recently been implicated in Scott syndrome, a rare congenital bleeding disorder caused by a defect in blood coagulation(Yu et al., 2015). In Ba/F3 platelet cells.

Ano6 was also found to be critical for Ca2+ dependent exposure of phosphatidylserine, which suggest that Ano6 is required for scramblase activity. However, recent report shows that Ano6 is a non-selective cation channel imply that Ano6 may have some new physiology function(Keckeis et al., 2017b).

1.3.2.6. ANO9

A previous report showed that ANO9 may act as a marker for poor prognosis in pancreatic cancer because ANO9 expression level increase was detected in most pancreatic cancer cell lines and pancreatic cancer patient tissue samples(Jun et al., 2017). Recently, Ano9 was identified as cAMP activated cation channel activity and may be associated with intestinal function(Kim et al., 2018).

1.3.2.7. ANO10

ANO10/TMEM16K belongs to a family of ion channels and phospholipid scramblases. Previous study showed that mutations in Ano10 was related to autosomal-recessive cerebellar ataxias associated with moderate gait ataxia, downbeat nystagmus, and

dysarthric speech(Nanetti et al., 2019). Affected individuals display severe cerebellar atrophy. Two of the mutations introduce premature stop codons, probably leading to null protein expression. The other mutation is a missense mutation, L510R, which is highly conserved among the Anos and lies in the sixth transmembrane domain within the DUF590 domain of unknown function. It remains especially uncertain whether Ano10 is an ion channel, because Ano10 and Ano8 constitute the most divergent branch of the anoctamin family(Duran and Hartzell, 2011).

2.Baroreceptor reflex

2.1. Overview

The baroreflex, also known as baroreceptor reflex, is one of the mechanisms that helps to maintain blood pressure at stable levels. The baroreflex is a rapid negative feedback loop. When the blood pressure increase, it will reflexively decrease the heart rate to bring back blood pressure to normal level. Once blood pressure decreases, it will inhibit baroreflex activation and causes heart rate

to increase and to restore blood pressure levels(Fernandez et al., 2015; Iliescu et al., 2014) (Figure 3).

The characteristics of baroreceptor reflex are as follows: (1) The appropriate stimulus is the stretch of blood vessel wall when blood pressure changes, not the arterial blood pressure itself; (2) The range of regulated arterial blood pressure is about 60~180mmHg; (3) Sensitive to sudden or fluctuating blood pressure change, but less sensitive to slow blood pressure changes; (4) carotid sinus sensitivity is higher than aortic arch; (5) it can elevate and decrease the blood pressure.

Baroreceptor reflexes do not play an important role in the long-term regulation of arterial blood pressure. In patients with chronic hypertension or experimental hypertensive animals, the baroreflex function cure is shifted to the right, called re-regulation of baroreflex(Parkin et al., 2016). It suggests that the working range of baroreceptor reflex changes in long-term hypertension. Arterial blood pressure also maintains a steady state at a relatively high level. Therefore, baroreflex cannot decrease blood pressure to a

normal level. In addition, clinicians use the carotid sinus to stimulate the carotid sinus and stimulate the vagus nerve through antihypertensive reflex to treat uncontrolled hypertension. Baroreflex adjustment is important for dealing with postural hypotension, such as control blood pressure to decrease on standing due to gravity(Low and Tomalia, 2015).

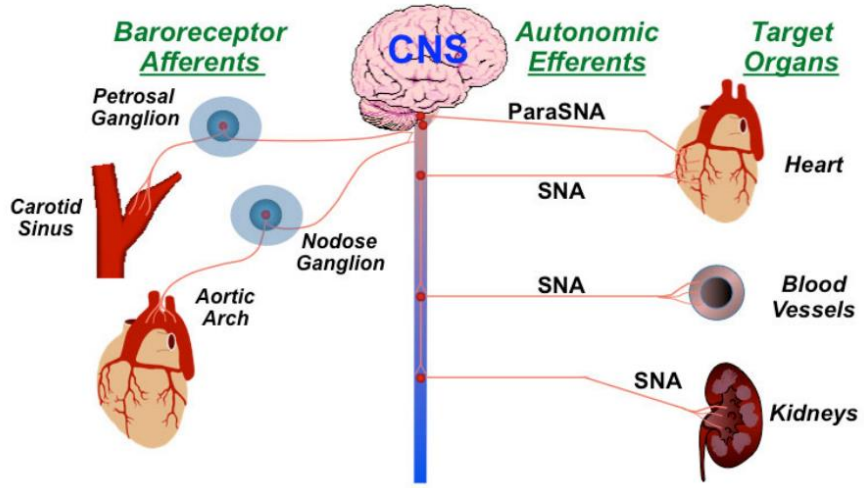

Figure 3. Mechanism of Baroreflex

The nodose is the somas where neurons project their mechanosensing afferent terminals into the carotid sinus and aortic arch. These neurons also project to the medulla. There the baroreceptor signals will cause increase parasympathetic and decrease sympathetic nerve activities with major effects on heart rate, cardiac function, vascular resistance, renal function and renin release. Reference from (Lu et al, 2009)

2.2. Baroreflex pathway

When increase or decrease in blood pressure occurs, the baroreceptors immediately can respond. The most important role is responding to sudden reductions in arterial pressure(Ichinose and Nishiyasu, 2012). This can occur, for example, when a person changes his position suddenly stands up or following blood loss (hemorrhage). This will cause a sudden decrease in mean blood pressure, pulse blood or both and result in decreased baroreceptor firing action potential. Under normal physiological state, the firing of baroreceptor can inhibit the outflow of sympathetic nerve from the medulla. Therefore, acute hypotension leads to the inhibition of sympathetic activity in the medulla oblongata and increases the sympathetic activity originated in the ventral medulla oblongata. These autonomic changes can cause vasoconstriction and tachycardia. The latter change increases cardiac output. Increased cardiac output and systemic vascular resistance lead to partial recovery of arterial pressure (Figure 4).

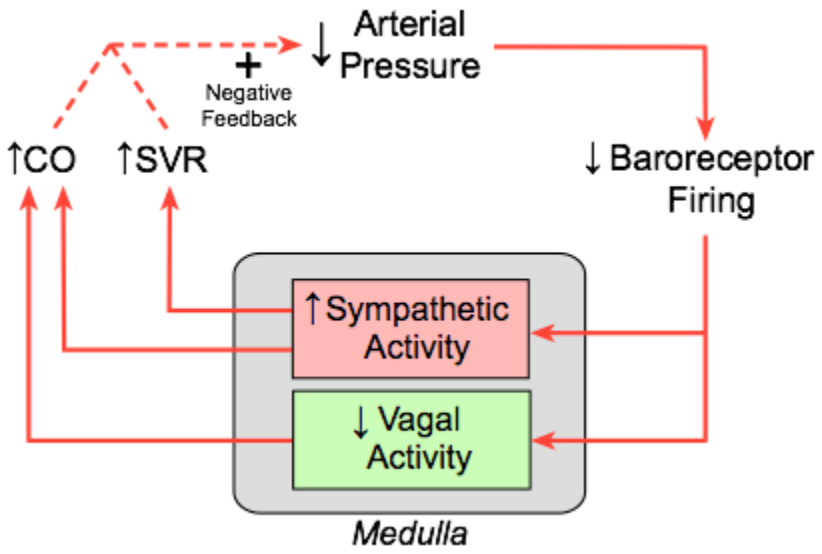

Figure 4. Baroreflex pathway

Arterial pressure decrease will decrease baroreceptor activity which will by reflex activate sympathetic system and inactivate parasympathetic system in the medulla. These finally increase cardiac output (CO) and systemic vascular resistance (SVR) act as a negative feedback to control blood pressure. Reference from (Klabunde, 2013).

2.3. Baroreceptors

The baroreflex system depends on the specialized neurons located in the wall of aorta and carotid sinus. The specialized neurons are baroreceptors which control changes in blood pressure and relay them to the medulla oblongata(Vasquez et al., 1997). Obviously, baroreceptors are stretch-sensitive receptors and respond to stretching of the blood vessel caused by increase of blood pressure. When blood pressure increases, the carotid and aortic sinuses are distended, which will cause increased stretch on baroreceptors. Then, the baroreceptors will fire more action potentials. Even at normal level blood pressure, some baroreceptors still report blood pressure information to the central system. Thus, the baroreflex is actively modulating autonomic activity: the parasympathetic and sympathetic nerves. Also, many individual baroreceptors are inactive at normal level blood pressure and only become activated when the blood pressure is changed. This is because the different stretch or pressure sensing threshold.

3. Candidates for Mechanosensitive ion channels in Baroreceptors

Because of the importance of baroreceptors in controlling blood pressure, many candidate genes of channels were suggested to be mechanosensitive channels responsible for baroreceptor function.

3.1. ENaC and ASIC2

DEG/ENaC family was first found in mutant *C. elegans* worms that are incapable of detecting gentle touch of their bodies. A variety of relevant genes were discovered(Bounoutas and Chalfie, 2007) (Figure 5). Each member of DEG/ENaC family has a pore region that is selective for sodium ion or some other ions. It is well known that the ENaCs are very important for whole-body sodium homeostasis. Previous reports showed that an ENaC subunit is found in the aortic baroreceptor nerve terminals, More importantly, the ENaC antagonist amiloride analogs can block baroreceptor activity which suggest that γENaC is a component of a

mechanosensitive channel complex at aorta(Drummond et al., 1998).

The acid-sensing ion channel 2 (ASIC2) is in a vertebrate member of the DEG/ENaC family which includes most channels that are exquisitely sensitive to extracellular pH change(Askwith et al., 2004). Interestingly, the ASIC2 subunit is least acid sensitive and show some mechanosensitve required for some mechanosensory processes in peripheral cutaneous and gastrointestinal nerves(Holzer, 2015). Lu and his colleagues(Lu et al., 2009) proved their hypothesis that ASIC2 is an important mechanosensitive sensor for aortic baroreceptor reflex and neurohumoral control of circulation.

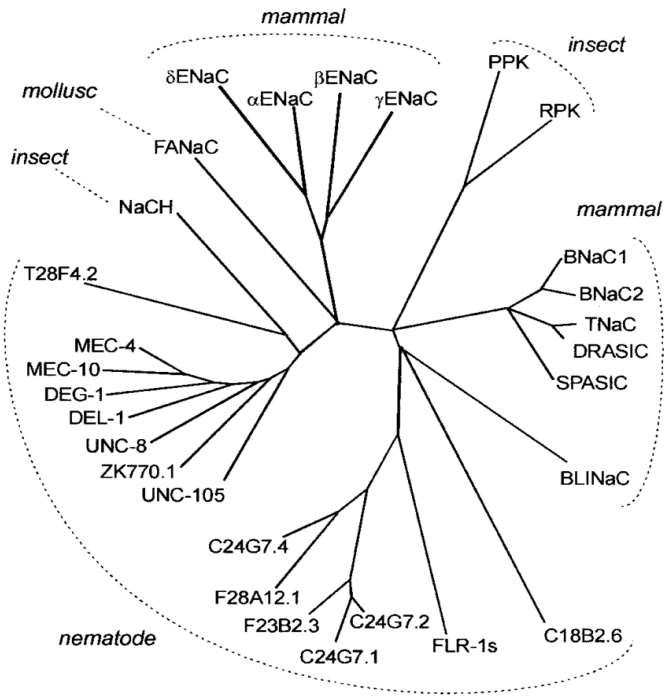

gene	protein isoforms	
ACCN1	BNaC1α/ BNC1/ MDEG1/ ASIC2a	BNaC1β/ MDEG2/ ASIC2b
ACCN2	BNaC2α/ ASIC1	BNaC2β/ ASIC1β
ACCN3	TNaC/ ASIC3/ DRASIC	
--	SPASIC/ ASIC4	

Figure 5. Phylogenetic tree of mouse Enac

Phylogenetic tree of the DEG/ENaC ion channel family, which contains proteins from nematodes, insects, mollusks, and mammals. Bottom, Members of the ENaC branch, with assigned human gene names and the protein isoforms resulting from alternative splicing. The various names of each isoform are separated by slashes. Reference from (Coscoy and Barbry, 2004)

3.2. TRPC5

Transient receptor potential (TRP) channels are a group of cation channels that act as cellular sensors to adapt to rapidly sense a variety of environmental stimuli including pain, heat, cold and taste(Bautista et al., 2007; Caterina et al., 2000; Caterina et al., 1999). According to sequence homology, the TRP channel superfamily can be divided into 6 subfamilies: vanilloid (TPRV), melastatin (TRPV), ankyrin (TRPA) and canonical (TRPC). Numerous reports already showed that some TRP channels are sensitive to various forms of mechanical stimuli such as membrane stretching, hypoosmolarity and fluid shear stress(Bautista et al., 2007). Previous reports suggested that TRPC5, TRPV2, TRPM4, TRPV4 can be directly activated by membrane stretching activates(Gomis et al., 2008; Loukin et al., 2010; Numata et al., 2007).

Membrane-stretching activated channels can be directly stimulated by mechanical stimulation and convert the mechanical force to electrical signals. These characteristics make these

channels become the candidates for mechanical sensors and mechanical transducers. Previous studies already demonstrated that TRPC5 is activated by hydrostatic pressure, hypo-osmolarity and membrane stretching(Gomis et al., 2008).

Recently, TRPC5 is reported to be expressed in baroreceptor neurons(Lau et al., 2016). Thus, TRPC5 is suggested to play a role in baroreceptor neurons as a pressure sensor. They observed a stretch-activated channel in the aortic baroreceptor neurons whose properties was very similar to TRPC5. Meanwhile, Trpc5 knock-out (KO) mice show the lower aortic depressor nerve and carotid sinus nerve activities. In addition, Trpc5 knock-out mice also displayed instability in daily blood pressure(Lau et al., 2016).

3.3. TRPV1

Because TRPV1 can be activated by capsaicin, it was initially known as the capsaicin receptor(Caterina et al., 1999). TRPV1 is a nonselective cation channel which can be activated by a vigorous exogenous and endogenous physical or chemical stimuli.

One of The best-known activators of TRPV1 are heat(when the temperature is more than 43°C (109°F)(Caterina et al., 1999). In addition, low pH, N-oleyl-dopamine, and N-arachidonoyl-dopamine also can activate TRPV1. TRPV1 are mostly expressed in nociceptive neurons in dorsal-root ganglia (DRG), thus considered to be a nociceptive marker(Caterina et al., 1997). TRPV1 also expressed in the nodose ganglia and visceral afferent fibers(Wang et al., 2017). Stimulation of TRPV1 afferent terminals can increase glutamate release to nucleus tractus soliarius neurons(Peters et al., 2010).

Sun and colleagues(Sun et al., 2009) showed the distribution of TRPV1 along the baroreceptive pathway and TRPV1-positive neurons. They also used resiniferatoxin, an ultrapotent analog of capsaicin, to ablate TRPV1-expressing primary afferent nerves and neurons to determine the contributions of TRPV1-expressing afferent neurons to the baroreflex function.

3.4. Piezos channel

Piezo proteins are the pore-forming subunits of mechanosensitive ion channels that can be directly gated by mechanical forces (membrane stretch and shear stress)(Coste et al., 2010) (Figure 5). Most vertebrates have two channel isoforms, Piezo1 and Piezo2. Piezo are very large proteins that contain more than 34 predicted transmembrane domains. When the piezo channel is open, the positively charged ions such as Na^+ and Ca^{2+} will flow into the cells. Piezo channels are very important for conversion of mechanical forces into biological signals.

Piezo2 is found in a subset of somatosensory neurons(Woo et al., 2015) and nodose ganglion (NG) neurons(Nonomura et al., 2017). The afferent from soma will project to several different organs throughout the whole body. Previous study already show that piezo2 are important for light-touch sensing, mechanical pain(Szczot et al., 2018) and media the respiratory system function(Nonomura et al., 2017). Recently, Zeng *et al(Zeng et al., 2018).* showed that PIEZO1 and PIEZO2 coordinately contribute

to the baroreflex in mice. They found Piezo1 and piezo2 expression in the cell body of NG. By using retrograde labeling and fluorescent *in situ* hybridization, they showed that PIEZO1 and PIEZO2 transcripts are sparsely expressed in the nodose-petrosal ganglion complex. However, deletion of either PIEZO1 or PIEZO2 alone cannot affect blood pressure (BP) or heart rate changes in response to phenylephrine or sodium nitroprusside treatment. Also Piezo channels are responsible for rapidly-activated currents. Only double KO of PIEZO1/PIEZO2 together cause baroreceptor impairment. These results showed that piezo channels play a critical role in baroreceptor reflex.

A

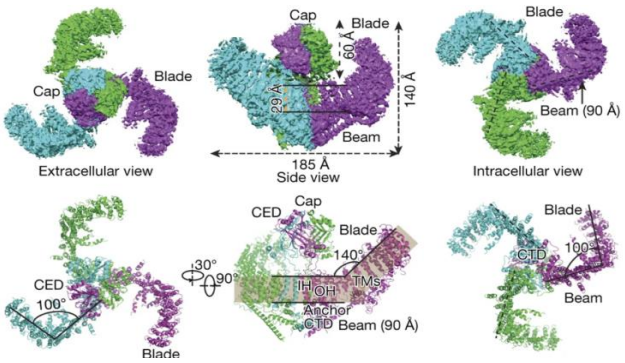

B

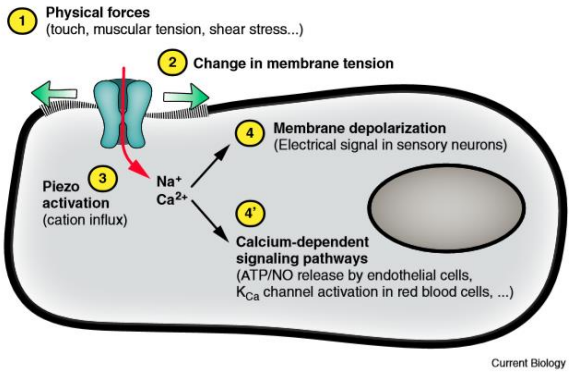

Figure 6. Piezos channel dependent mechanotransduction

A. Overall structure of Piezo1. Reference from(Wang et al., 2019)

B. Different kinds of mechanical stimuli such as touch, tension shear stress exerted on cells induce changes in plasma membrane tension, eliciting Piezo channel opening. This will cause cation influx which can trigger sensory neuron firing or activation of intracellular calcium signaling pathways. Reference from (Parpaite and Coste, 2017)

3.5. TMEM150c (TTN3) channel

TTN3 is a cation channel activated by mechanical stimuli in the heterologous system. Its mechanosensitivity is blocked by known MA channel blockers such as gadolinium, GsMTx4, and FM1-43(Hong et al., 2016). TTN3 was found to be highly expressed in DRG, pancreas, and epididymis (Figure 7). Therefore, TTN3 might play some roles in these organs, including cancer-related functions. In DRG, because TTN3 inactivates slowly, it is classified as slowly-adapting (SA) MA channel(Hong et al., 2016). It was reported that TTN3 is expressed in muscle spindle afferents and mediate muscle coordination. In pancreases, we also found that TTN3 is expressed in the beta cells and participate in sensing and regulating insulin release. Recently, we found that TTN3 is also expressed in nodose ganglia and its terminals in the aorta. Thus, we hypothesized that TTN3, as an MA ion channel, might be actively involved in detecting AP changes in baroreceptors.

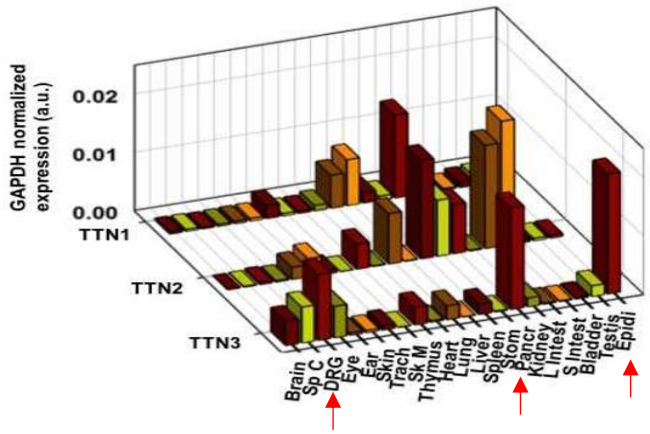

Figure 7. TTN3 expression level in different tissue

mRNA transcript levels of TTN3 in various mouse tissue organs. Note that TTN3 is highly expressed in DRG, pancreas, and epididymis Reference from(Hong et al., 2016).

4 . Anoctamins in nociception

In mammals, pain-producing stimuli are detected by nociceptive nerves whose somas are located in the DRG and extend peripheral and central processes to reach their target organs and the spinal cord. DRG neurons divided into three groups according to their size. Large, middle and small size DRG neurons. Unmyelinated C fiber neurons comprise a major class of nociceptors that are implicated in pain(Yam et al., 2018). They can further subdivide to the peptidergic and non-peptidergic types. The latter binds the IB4 isolectin and expresses G protein-coupled receptors of the Mrg family(La et al., 2016).

Nociceptive transduction in DRG neurons is achieved through the activation of specific classes of ion channels, which are the molecular sensors that may detect sensory stimuli and convert them into electrical signals(Oh and Jung, 2016). Ano1 in DRG neurons is known to be activated by physiological intracellular $Ca2^{+}$, which depolarizes the sensory neurons(Cho et al., 2012). In ANO1 conditional knockout mice DRG neurons, heat-activated

chloride currents are reduced. More importantly, mice lacking ANO1 in DRG neurons are significantly insensitive to noxious heat, suggesting that ANO1 mediates acute thermal pain(Cho et al., 2012). Also, ANO3 (TMEM16C) appears to contribute to nociception. ANO3 is associated with a sodium-activated potassium (Slack) channel(Huang et al., 2013). ANO3 is expressed in isolectin B4-positive DRG neurons and genetic ablation of ANO3 reduces the expression of Slack channel as well as its currents. ANO3 activity would dampen the excitability of nociceptors. Indeed, ANO3-ablated rats reveal nociceptive hypersensitivity.

5. cAMP-PKA signaling pathway in DRG

The cyclic nucleotide signaling, including the cAMP-PKA and cGMP-PKG pathways, has been well known to play critical roles in regulating cellular growth, metabolism and many other intracellular processes(Serezani et al., 2008; Stork and Schmitt, 2002; Yamamizu and Yamashita, 2011). In addition, many studies

have demonstrated the involvement of cAMP-PKA pathway in inflammatory(Lewin and Walters, 1999; Malmberg et al., 1997), neuropathic(Huang et al., 2012c) and bone cancer pain(Zhu et al., 2016). cAMP has been implicated in nociception. The inhibition of the cAMP pathway by blocking the activities of adenylyl cyclase and protein kinase A (PKA) has been found to prevent chronic pain in animal models(Kim et al., 2007).

Neuronal hyperexcitability may be associated with cAMP signaling in the context of peripheral tissue injury. Numerous studies have implicated the cAMP-PKA pathway in producing hyperexcitability of DRG sensory neurons(Aley and Levine, 1999; Taiwo et al., 1989). Thus, the cAMP-PKA pathway regulates sensory neuron excitability after injury, which involves several members of TRP channels, sodium channels and potassium channels(Li et al., 2019) .

THE PURPOSE OF STUDY

Baroreceptors are sense organs scattered around the aorta, common carotid artery, and carotid sinus for detecting changes of AP. Baroreceptors are mechanosensitive; therefore, mechanosensitive channels may transduce the pressure change to electrical signals in baroreceptors. However, the mechanosensitive ion channels for baroreceptors are not clear.

Because TTN3 is a mechanosensitive channel, it is possible for TTN3 to mediate baroreceptor functions. Therefore, the aim of this study is to investigate the role of TTN3 in the baroreceptor.

In addition, TMEM16 or Anoctamin (ANO) gene family consists of ten isoforms. Although biophysical and physiological properties of some members of Anoctamin family are well described, the function of TMEM16H (ANO8) is unclear. Thus, the second aim of the present study is to determine whether ANO8 is a channel. If it is a channel, its activation mechanism as well as ion selectivity is determined.

METHODS

1.Cell culture and transfection

HEK 293T cells were incubated in Dulbecco's modified Eagle medium (DMEM) with 10% fetal bovine serum (FBS), 2mM L-glutamine, 1mM sodium pyruvate, and 100U/ml penicillin/ streptomycin. The cells were maintained at 37℃, 5% CO_2. The cells were transfected with mAno8 cDNA with Lipofetamine 3000 reagent (Invitrogen). Path clamp experiments were performed 48-72h hours after gene transfection.

2. Patch clamp

Whole-cell recordings were performed using a voltage clamp technique with Axopathch 200B amplifier as descried previously(Cho et al., 2012; Yang et al., 2008b). Briefly, whole-cell voltage-clamp recordings were performed at room temperature and recorded using Axopatch 200B amplifier (Molecular Devices). Pipettes were pulled from borosilicate glass capillaries with a P-97

puller (Sutter Instrument). The pipette solution contained 140 mM KCl, 2 mM $CaCl_2$, 2 mM MgCl2, 10 mM HEPES, and adjusted to pH of 7.2 with KOH. The bath solution was 140 mM NaCl, 2 mM CaCl2, 2 mM MgCl2, 10 mM HEPES, and adjusted to pH 7.2 with NaOH. The osmolarity of all solution was adjusted to 300 mOsm with the application of D-Mannitol. Whole-cell currents were recording after formation of a gigaseal (> 1GΩ) and breaking the cell membrane, making whole-cell configuration.

Different Ca^{2+} concentration pipette was prepared with 10 mM EGTA to make the free 1.0 and 10 M Ca^{2+}, final free Ca^{2+} was calculated by using WEBMAXC (http://www.stanford.edu/~cpatton/webmaxcS.htm).

3.Mechanical stimulation

Mechanical stimulation, step mechanical stimuli were applied to the HEK cell surface with a fire-polished glass pipette as described previously. From the initial position at the surface of an NG cell, the glass probe was moved forward from 2.5 to 7.2 mm in

0.42 mm increments. The duration of the mechanical stimuli was set at 600 ms. The movement of the glass probe was made with a micromanipulator (NC4, Kleindiek Nanotechnik).

4.Animals and *Ttn3*^{cre} mice

All mice procedures were approved by the Institute of Laboratory Animal Resources of the Seoul National University and the Korea Institute of Science and Technology. Mice less than four were housed in each cage on a 12 h light-dark cycle with free access to food and water. The healthy condition of all mouse was regularly checked. Seven to eight-week-old mice (20-24 g) were used for all experiments. Male C57BL/6J (wild type) mice or *Ttn3*$^{-/-}$ mice were used throughout the paper. The generation of *Ttn3*$^{-/-}$ mice was described elsewhere (Hong et al., 2016).

The *Ttn3*^{cre} mice were generated by homologous recombination (or homology-directed repair: HDR) using the CRISPR/Cas9 system at the Macrogen Co (Seoul, Korea). Briefly, the homology regions from the BAC clone containing *Tmem150c*

locus were cloned into a plasmid. The start codon sequences of Tmem150c were targeted for insertion of *Cre* recombinase gene. The SV40 poly(A) signal sequences were located just after the *Cre* gene. The plasmid including 1 kb homology arms was utilized as an HDR donor, which was verified by enzymatic digestion and sequencing. To avoid cleavage of the HDR donor by CRISPR/Cas9-mediated site-specific double-strand break, the HDR donor contains a silent mutation on the selected sequence of guide RNA. FVB/N stud males were mated to Super-ovulated FVB/N mice. Fertilized zygotes were collected from oviducts. Cas9 protein, synthetic single-guide RNA, and the HDR donor were mixed and injected into the pronucleus of fertilized zygotes. The injected zygotes were implanted into oviducts of pseudopregnant CD1 mice. The knock-in mouse was backcrossed with C57Bl/6J strain, and two of these knock-in lines were crossed to get reporter mice. All $Ttn3^{cre}$ mice used here were maintained as a hybrid FVB x C57Bl/6J mice. Founder pups and offsprings were genotyped for confirming the presence of the knock-in gene by

PCR (expected size 1741 bp).

5.Immunofluorescence

The immunostaining methods were similar to those described previously (Cho et al., 2012; Yang et al., 2008b). Briefly, after anesthetizing mice deeply by isoflurane, mice were perfused with 4% paraformaldehyde (PFA) in phosphate buffered solution (PBS). The left NG and aortic arches were isolated from adult wild-type, *Ttn3*$^{-/-}$, and AAV-hsyn-*Ttn3*-mCherry treated mice. The tissues were fixed with 4% paraformaldehyde and frozen in Tissue-Tek O.C.T. The cryosections in 10-μm thickness were incubated with blocking buffer (4% bovine serum albumin in phosphate buffer saline with Tween 20) for 30 min, and with polyclonal TTN3 (1:700), PGP9.5 (1:500), or NFH (1:500) antiserum overnight at 4^0C. After being washed for 15 min, the samples were incubated with Alexa Fluor 488–conjugated goat antibody to rabbit (A11008, Life Technology, 1:800), Alexa Fluor 546–conjugated goat antibody to mouse (A11003, Invitrogen, 1:600), or Alexa Fluor 555–conjugated goat antibody to chicken (A21437, Life

Technology, 1:800) at room temperature for 1 h. The nucleus was stained using Hoechst 33342 for 10 min (H3570, Thermofisher Scientific, 1:2000). Labeled sections were imaged using a confocal microscope (LSM700; Carl Zeiss).

6.RT-PCR

Diversified mouse organs were isolated from C57BL/6J mice (7 weeks). mRNA expressions of *Ano8* and *Gapdh* were detected with RT-PCR. Total RNA of different tissues were extracted by using a Total RNA Extraction Kit (Easy-spin™, Intron) and reverse transcribed into cDNA using Reverse Transcriptase (GoScript™, Promega). Target genes were amplified by using DreamTaq DNA Polymerases (Thermo-Fisher). mRNA expressions of Ano1, Ano8, Ano9 and Trpv1 in DRG were detected with RT-PCR. The primers used for PCR are:

Primer	Forward	Reverse
Ano1	TTGGTGAGAAGGTTGGCCTG	CCTTGACAGCTTCCTCC
Ano8	AGGCCAGCCAATCATTCG	CTTGTAGGTAGCTCTGCCC
Ano9	TGGTTCCTCGCAAGGCTAAG	GCACAGGGCAAAATGCTCAA
Gapdh	GTGAAGGTCGGTGTGACCGA	CCCATCACAAACATGGGGGCA
Trpv1	ACCACGGCTGCTTACTATCG	GTGTCACTACGGCTGTGGAA

7.Dil-labeling of aortic BR neurons

Mice were deeply anesthetized with 50 μl of Zoletil 100 (Virbac) and Rompun (Bayer) cocktail (ratio 3:2). Mice have ventilated with a small animal ventilator (SAR-1000, CWE). After the sternum was cut to expose the chest, we applied Dil (1,1'-dioctadecyl-3,3,3',3'-tetramethylindocarbocyanine perchlorate, Thermo-Fisher) crystals (25 mg/ml,1 μl) to the adventitia of aortic arch using a nanoinjector device (Nanoliter 2010, World Precision Instruments). After injection, the area was then covered with parafilm and a silicone gel (Kwik-Sil, World Precision Instruments). Mice were allowed to recover for 6-7 days so that Dil can efficiently trace to neurons in NG.

8.Primary culture of NG or DRG neurons

Left NG was dissected from WT or *Ttn3*$^{-/-}$ mice after anesthetized with 50 μl of Zoletil 100 (Virbac) and Rompun (Bayer) cocktail (ratio 3:2). The NG was collected in the culture solution containing DMEM and F-12 solution, 10% BSA, 50-100 ng/ml nerve growth factor (Alomon) and 100 units per ml of penicillin/streptomycin. The NG was incubated for 30 min in a 37^{0}C DMEM F-12 containing 1mg/ml collagenase IA (Sigma). NG was washed 3 times with Hank's solution (Mg^{2+}- and Ca^{2+}-free) and digested in 0.125mg/ml trypsin (Roche Diagnostics) for 30 min at 37^{0}C. The trypsinized cells were centrifuged at 100g for 10 min, gently triturated with a fire-polished Pasteur pipette, and plated onto round glass coverslips (Fisher), which had been previously treated with poly-L-lysine (0.5 mg ml−1), in small Petri dishes (35 × 12 mm). Cells were then placed in a 37°C incubator supplied with 95% air/5% CO2 atmosphere. Electrophysiological experiments were performed after 2-3 days of incubation.

9.Tissue clearing and staining

Ttn3^{cre} mice were injected with AAV DJ-EF1α-DIO-eYFP into the right NG. 4 weeks later, the mice were anesthetized deeply with isoflurane and perfused with 4% PFA. Under a dissection microscope, the aortic arch was isolated. The upper part of the aortic arch was further dissected for clearing and staining. The clearing process was described elsewhere (Susaki et al., 2015). Briefly, isolated aorta was fixed in 4% PFA for 1 day and incubated in CUBIC-1 solution at 37ºC for 7 days for clearing. The samples were washed in 1xPBS solution three times for longer than 2 h and incubated in 1xPBS containing 3% normal donkey serum solution and anti-NFH antibody (1:200) at 23^{0}C for 3 days. After 1-day washing in 1xPBS, the samples were immersed in 1x PBS containing 3% normal donkey serum and Alexa 594-conjuated anti-chicken antibody (Jackson ImmunoResearch, 703-585-115; 1:500 dilution) and Alexa 647-conjugated anti-GFP primary antibody (Thermo Fisher Scientific, A-31852; 1:250 dilution) at 23ºC for 3 days. Samples were washed in 1xPBS for 2 h, incubated

in 1xPBS with 1:5,000 DAPI (Thermo Scientific, 62248) for 2 h, and immersed in CUBIC-2 solution (Susaki et al., 2015) overnight for refractive index-matching. The samples were then mounted on a slide with CUBIC-2 solution and imaged with a confocal microscope (LSM 880, ZEISS).

10.Recoding of aortic depressor nerve activity

Ex-vivo recording of ADN was described elsewhere (Sato et al., 1999). Briefly, mice were anesthetized with 1.5% isoflurane. After exposing the aortic arch in the chest, the cardiac end of the ascending aorta, brachiocephalic trunk, and both the left and right common carotid arteries were ligated, carefully dissected out from the body, and placed into an oxygenated bath solution containing 123 mM NaCl, 3.5 mM KCl, 0.7 mM $MgSO_4$, 1.7 mM NaH_2PO_4, 2.0 mM $CaCl_2$, 9.5 mM mannitol, 5.5 mM glucose, 7.5 mM sucrose, and 10 HEPES (pH 7.40). A small glass tube was inserted into the other end of the aorta. The aorta covering the glass tube was tied tightly. The glass tube was connected to a fluid-filled pressure

transducer and a syringe for adjusting the pressure inside the aorta. The output signal of the pressure transducer was amplified and fed into a computer.

Nerve activity of the ADN was recorded using a suction electrode with a tip diameter of 70 μm filled with the bath solution. Suctions were repeated until neuronal activities were identified. After 10 min stabilization of ADN activity, the pressure steps of 0 mmHg, 50 mmHg, 100 mmHg and 150 mmHg were given to the isolated aortic arch. Each pressure stimulation lasted for ~30 sec with 3 min interval. Electrical signals in the suction electrode were amplified with ISO-80 (World Precision Instruments), filtered at 1 kHz, digitized at a sampling rate of 10 kHz with Digidata 1322 (Molecular Devices), and stored in a computer. The stored traces were later analyzed using the pClamp software version 10.0 (Molecular Devices). Spikes with the voltage amplitude greater than one standard deviation of the noise were counted as action potentials.

11. 24-hour recording of blood pressure and heart rate

The 24-hour arterial pressure recording method was modified from a previous protocol (Butz and Davisson, 2001). Briefly, WT or TTN3$^{-/-}$ mice were initially anesthetized under 4% isoflurane followed by 1.5% isoflurane for maintaining the anesthetic condition. A catheter attached to a telemetric pressure transducer (PA-C10, Data Science International) was inserted into the right common carotid artery. The telemetric pressure transducer was embedded in the abdominal region subcutaneously. After 6 days of recovery, 24 h arterial pressure and heart rate were recorded in conscious, freely moving mice by the DSI Dataquest telemetry system (Data Science International) at a sampling rate of 500 Hz for 10-seconds in every 5 minutes.

12.Whole-body plethysmography test

The procedure to assess respiratory functions using whole-body plethysmography has been described elsewhere(Mailhot-Larouche et al., 2018). In brief, each mouse was acclimated for 30

min in the restrainer, then placed into the thoracic chamber. A bias flow of 0.5 L/min was given to the mouse. The animal was kept calm for 5 min, then the recording is started. Each session lasted 20mins. Mice were then released from the restrainer and returned to their housing cage. Traces and recording parameters were automatically recorded and stored in a computer.

13.Baroreflex response test

Mice were anesthetized under 1.5% isoflurane, a heparinized saline-filled (50 Unit/ml) tube was inserted into the femoral vein of the mice. The other end of the tube was plugged, tunneled subcutaneously, and sutured at the dorsal face of the neck. After the mice recovered for 3 days, bolus injections of phenylephrine (4 μl/kg, Sigma) were made to test the baroreflex sensitivity by checking the changes in arterial pressure (Braga et al., 2008). The baroreflex sensitivity is calculated as △BPM divided by △mmHg.

14.Chemogenetic inhibition or activation of TTN3+ neurons

Selective inhibition or activation of TTN3+ neurons in NG was

achieved using the DREADD system. *Ttn3*^{cre} mice were anesthetized under 1.5% isoflurane, and the right and left nodose ganglia were surgically exposed. A micropipette containing AAV-hsyn-DIO-mCherry, AAV-hsyn-DIO-hM4Di-mCherry or AAV-hsyn-DIO-hM3Dq-mCherry was inserted into NG (Lerch et al., 2012). Animals were allowed to recover for 4 weeks prior to the telemetric recording of AP and HR. Mice were allowed to adapt to the intraperitoneal CNO (2 mg/kg, 10 ul) injection by injecting saline once a day for 3 days before the CNO experiments. BP and HR signals were then recorded 15 min (as a baseline) before and 45 min after the intraperitoneal injections. Data were normalized to the 15-min baseline. After the completion of experiments, mice were perfused and nodose ganglia were collected to check the mCherry expression. Mice without hM3Dq or hM4Di expression were excluded from the analysis.

15.SiRNA

For efficiently knock down Ano8, we designed two siRNAs

(Bioneer, Korea) that target different region of the Ano8 transcript. The targeted siRNA sequence was:

Ano8_siRNA1: CUGUUCUACAUCGGCUUCU=tt(1-AS)

AGAAGCCGAUGUAGAACAG=tt(1-AA)

Ano8_siRNA2: CUGAAUCGUCUCAUGAAGU=TT(2-AS)

ACUUCAUGAGACGAUUCAG=TT(2-AA)

16.AAV infection of nodose ganglion or DRG

TTN3-/- mice were anesthetized under 1.5% isoflurane, and the right and left nodose ganglia were surgically exposed. A micropipette containing AAV-hsyn-mCherry or AAV-hsyn-TTN3-mCherry was inserted into the NG (Lerch et al., 2012). The virus solution (100 nL) was injected using a Nanoliter 2010, (World Precision Instruments). Animals were allowed to recover for 3 weeks prior to the recording of AP, HR, and baroreflex sensitivity.

DRG injection of AAV was performed as described previously(Simonetti et al., 2014). Briefly, mice were anesthetized under 1.5% isoflurane, DRG (left L4-L5) were surgically exposed.

A micropipette containing AAV-control or AAV-shANO8 was inserted into the DRG. The virus solution was injected using a Nanoliter 2010, (World Precision Instruments). Animals were allowed to recover for 4 weeks prior to behavior test.

17.Formalin induced pain behavioral test

The process of formalin test was similar to those described previously(Malmberg and Yaksh, 1992), Briefly. 20ul of 5% formalin solution was subcutaneously injected into the left hind paw by using a 30-gaguge needle. The mice were put in a transparent chamber for mouse behavioral video recording. Licking of the formalin-injected paw was considered as a nociceptive behavior. The time spent on licking was analysis in each 5 mins of one hour.

18.c-Fos immune-positive neurons counting

After formalin test, mice were sacrificed and perfused with PFA. The spinal cords was took out for immunohistochemical analysis. All the sections were counterstained with DAPI for cell nuclear

visualization. Four nonadjacent sections from the L4–L5 lumbar spinal cord from each mouse were randomly selected before the examination of c-Fos. The images of c-Fos in the dorsal horn ipsilateral to the formalin-injected hind paw were evaluated. When c-Fos staining in a cell was colocalized with nuclear staining (DAPI), the cell was counted as c-Fos-positive. The numbers of c-Fos-positive cells in dorsal horn were manually counted.

19.Statistical analysis

Data in the figures are all shown as a mean ± SEM. To compare multiple means, One-way ANOVA was used with Tukey's post-hoc test. Two-tailed Student's t test was used to compare two means. $P < 0.05$ considered as significant.

All statistical analyses were performed by using Graphpad prism version 7.0. Data in the figures are all shown as a mean ± SEM. To compare multiple means, One-way ANOVA was used with Tukey's post-hoc test. Two-tailed Student's t test was used to compare two means. $P < 0.05$ considered as significant.

RESULTS

1.TTN3 expresses in baroreceptor neurons

Because the somas of aortic baroreceptors are located in NG. So We first examined the presence of TTN3 in NG by staining with TTN3 antibody, heavy chain neurofilament (NFH), a marker for myelinated axons (Nixon and Shea, 1992; Wilkinson et al., 1989). Shown in Figure 8A, TTN3-positive neurons were found in NG neurons. These TTN3-positive cells were largely colocalized with NFH and However, TTN3-positive neurons were not observed in NG of *Ttn3*$^{-/-}$ mice (Figure 8A).

Because the afferent nerves that in NG also will project to several organs such as aorta, lung and gastrointestinal tracts (Brierley et al., 2012; Carr and Undem, 2003; Donoghue et al., 1982), but I just want to focus on the NG neurons that innervate in aortic arch only, So I inject a fluorescent dye, Dil (1,1'-dioctadecyl-3,3,3',3'-tetramethylindocarbocyanine perchlorate, 2.5 mg/ml) to the adventitia of the aortic arches of mice (Figure 8B). After seven days of recovery, NG neurons were primary cultured and stained

with TTN3 antibody. As shown in (Figure 8A), Dil-positive neurons were found in NG, which were also positive to TTN3. These results indicate that TTN3 was expressed in baroreceptors neurons of NG.

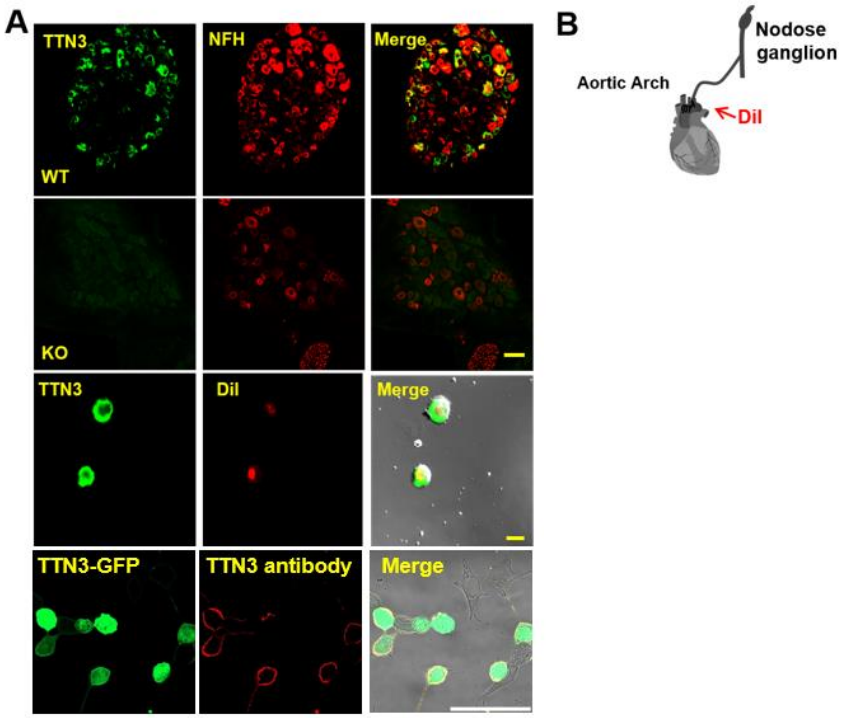

Figure 8. TTN3 was expressed in baroreceptors neurons of NG

(A)Immunofluorescent images of TTN3 in nodose ganglia isolated from wild-type (WT) and Ttn3-/- mice and expression of TTN3 in Dil-positive cells. The nodose ganglion (NG) neurons were stained with neurofilament H (NFH), a marker for myelinated nerve fibers. Bottom:TTN3 antibody confirm. Scale bar represents 50 μm

(B) Schematic diagram showing injection of the tracer Dil into the aortic arch adventitia to selectively label aortic arch-projecting neurons in the nodose ganglia.

2. TTN3 is responsible for SA MA currents in baroreceptor neurons

As we know, TTN3 is an MA channel with slow inactivation kinetics (Hong et al., 2016). And now we TTN3 is expressed in baroreceptors neurons, So Dil-positive NG neurons should retain MA currents property. Patch clamp experiments was performed with mechanical pulses (2.5~7.2-um indentation for 600 ms) application to DiI-positive NG neurons (Figure 9A). After application of mechanical step stimuli, three-different types of MA currents was observed. According to the inactivation kinetics, the MA currents in Dil-positive NG neurons could be also categorized to three groups as observed in Dorsal-root ganglion neurons; rapidly-adapting (RA) (t_i = 4.3 ± 0.5 ms, n = 19), intermediately-adapting (IA) (t_i = 22.1 ± 1.7 ms, n = 16), and slowly-adapting (SA) currents (t_i = 127.9 ± 21.8 ms, n = 20) (Figure 8B, C). Among the 72 aorta-innervated NG neurons, RA, IA, and SA-type neurons were 26.4, 22.2, and 27.8%, respectively (Figure 9B, C). The other neurons (23.6% of the tested neurons) showed no response to the

mechanical stimuli. We then repeated testing the mechanosensitivity of Dil-positive NG neurons isolated from *Ttn3*$^{-/-}$ mice. The proportion of neurons with SA currents was markedly reduced to 5.7% (Figure 9B, C). The proportions of RA and IA currents were not changed. However, the proportion of Dil-positive NG neurons with no response to the mechanical step stimuli increased in *Ttn3*$^{-/-}$ mice, which is conceivable because of the reduction in the SA NG neurons. These results suggest that TTN3 is functional as a SA MA channel in aortic baroreceptors.

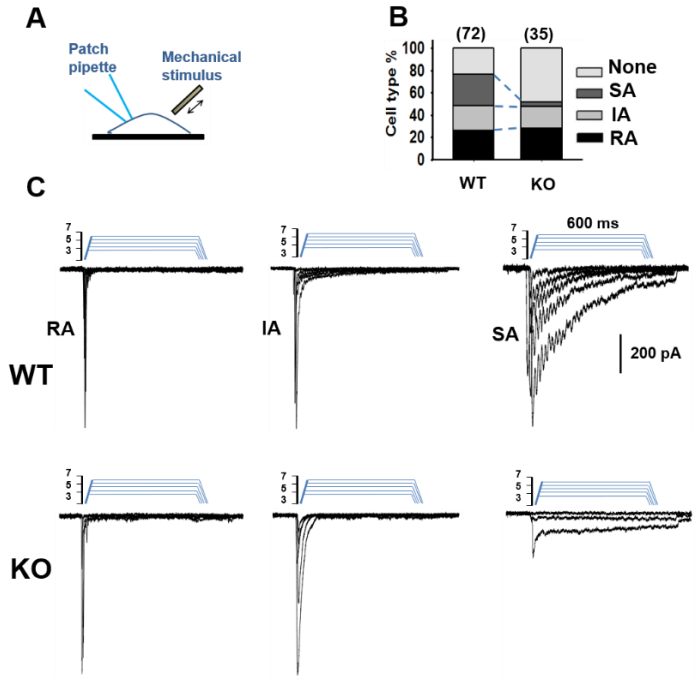

Figure 9. TTN3 is responsible for slowly-adapting mechanically-activated currents in aortic-arch projecting nodose-ganglion neurons

(A) Schematic diagram showing mechanical stimulation of DiI-positive NG neurons.

(B) Summary histogram illustrating three types of mechanically-activated currents characterized in aortic arch-projecting NG neurons based on inactivation kinetics. Intermediate-adapting (IA), rapidly adapting (RA), slowly-adapting (SA) mechanically-activated currents. (C) Representative traces of three types of mechanically-activated currents in DiI-positive NG neurons isolated from wild-type (WT) and Ttn3-/- (KO) mice. Probe displacement is illustrated above traces.

3. TTN3 is expressed on ADN in the aortic arch

Now I know the TTN3 was express the baroreceptor neuron body, for further confirm whether TTN3 is localized at the terminals of the aortic depressor nerve in the aortic arch. we expressed eYFP on the *Ttn3* promotor in NG neurons. For this, we generated *Cre*-transgenic mice at *Ttn3* promoter region (*Ttn3*^{Cre} mice) and inject A adeno-associated virus (AAV) carrying EF1a-DIO-eYFP (AAVDJ-EF1α-DIO-eYFP) was infected to the right NG of *Ttn3*^{Cre} mice (Figure 10A). To visualize the entry of nerve terminals in the aorta, a piece of the aortic arch was cut, fixed with paraformaldehyde, cleared with electroporation, and stained with anti-eYFP and NFH (Susaki et al., 2014; Susaki et al., 2015). Shown in Figure 10B, the eYFP-positive nerve fibers were spread over the adventitia of aorta, co-localizing with NFH. The eYFP-positive fibers were coiled and tortuous in a complex manner such that they formed a nerve plexus and arborized along the adventitia of the aorta. The discoid or ‘club’ ending form of eYFP-positive fibers spread along the adventitia but not penetrated to the media

of the aorta. This pattern of nerve terminals was unique in myelinated baroreceptor nerve fibers in the aortic arch in rat and mice (Doan et al., 2004; Krauhs, 1979; Song et al., 2012). These results showed that TTN3 is expressed at baroreceptor nerve terminals where the mechanotransduction occurs.

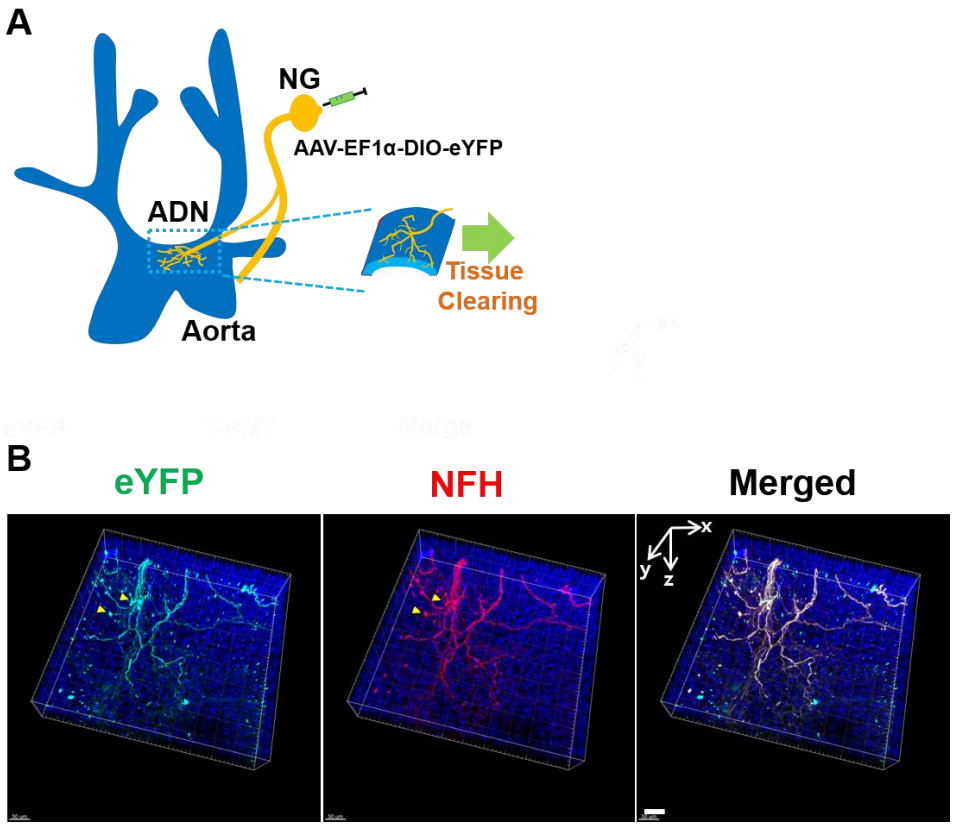

Figure 10. TTN3 is present at the site of mechanotransduction in baroreceptor nerve terminals

(A) Schematic illustration of clearing aortic depressor nerve (ADN) attached to the aortic arch. AAV DJ-EF1α-DIO-eYFP was injected into the right nodose ganglion of ttn3-cre mice and the transverse arch was cut off for clearing and imaing.

(B) 3D-reconstructed images of ADN terminals stained with EYFP (left), NFH(middle) and two color merge(right). Nerve plexus and terminals was shown by yellow triangle mark.Scale bar represents 50 μm.

4. TTN3 is required for pressure-evoked action potentials in ADN

Because TTN3 is an MA channel expressed in nerve terminals of the aortic depressor nerve (ADN), So the change of pressure in the aortic arch may active TTN3. To prove this, the aortic arch along with ADN attached to the aorta was isolated and the neural activity of AND was recorded. In this preparation, we injected saline to the thoracic end of the aorta while the cardiac end of the aorta and arterial branches were tied to make pressure change (Figure 11). When the aortic arch was pressurized at, 100, and 150 mmHg, the nerve fibers discharged action potentials in response to the intra-aortic pressures. The nerve activity increased as the pressure increased from 100 to 150 mmHg with the slope of 0.91 ± 0.05 spikes/mmHg (n = 8) in WT mice (Figure 12A, B). In addition, fairly high background activity of ADN of WT mice was observed (41.8 ± 5.2 spikes/sec, n = 8) at 0 mmHg intra-aortic pressure (Figure 12A, B). In contrast, the ADN activities of *Ttn3*$^{-/-}$ mice were markedly reduced at all pressures tested. The slope of

ADN sensitivity was also significantly reduced in *Ttn3*$^{-/-}$ mice (0.60 ± 0.12 spikes/mmHg, n = 8). In addition, the baseline activity of ADN of *Ttn3*$^{-/-}$ mice was significantly lower (12.7 ± 3.3 spikes/sec, n = 8) than those of the WT mice (Figure 12B, C). These data clearly indicate that TTN3 is functional in sensing changes of pressures in the aortic arch.

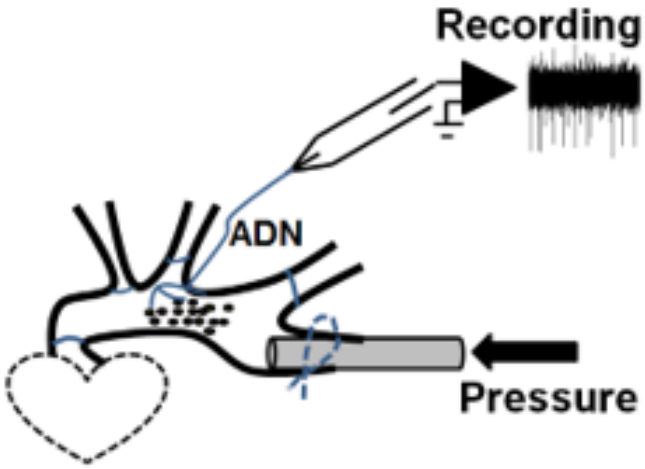

Figure 11. Schematic illustration of ex vivo recording from isolated aortic depressor nerve (ADN) attached to the aortic arch.

A glass tube was inserted to the thoracic aortic end and tightly tied with surgical sutures. Other branches of the aortic arch were also ligated to prevent a leak

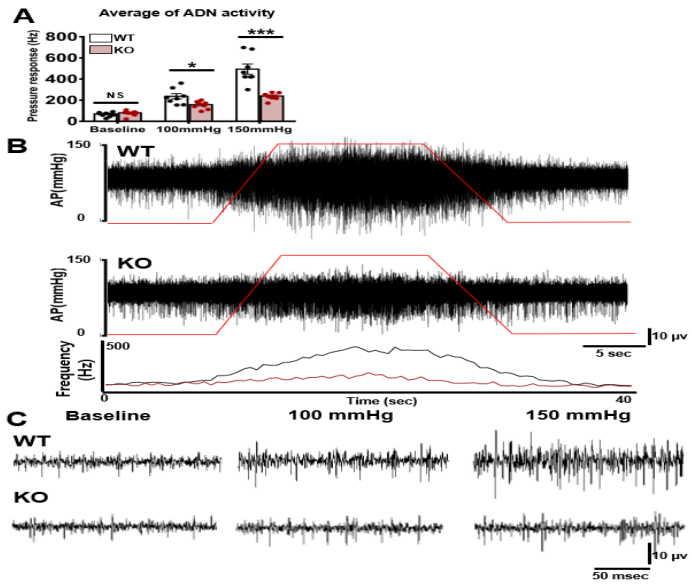

Figure 12. TTN3 is required for pressure-evoked action potentials in aortic depressor nerve

(A) Summary of ADN activities of WT (n = 8) and *Ttn3*$^{-/-}$ mice (n = 8) in response to the intra-aortic pressures. The slopes of the pressure-response curves of WT and *Ttn3*$^{-/-}$ mice represent the baroreceptor sensitivity, and were obtained with the ratio between spike frequency and pressure. (* $p < 0.05$, *** $p < 0.001$. Student's t-test)

(B) Representative traces of multi-unit activities in response to intra-aortic pressures in WT (top) and *Ttn3*$^{-/-}$ (middle) mice. The bottom panel shows the number of spikes per second before, during and after application of intra-aortic pressure.

(C) Same as in (B), with recordings at each pressure level shown in details.

5. TTN3-/- mice show hypertension, tachycardia, and AP instability

If TTN3 acts as a molecular sensor for detecting a pressure change in baroreceptors, the genetic ablation of *Ttn3* would affect AP and heart rate (HR). We, therefore, recorded ambient APs and HRs of freely moving mice of both genotypes for 24 hours continuously using a telemetric device. As expected for baroreceptor denervation (James and Potter, 1999), the 24-h ambient APs of WT mice were stable throughout the recording time (Figure 13A). Diurnal change in APs of *Ttn3*$^{-/-}$ mice was like that of the WT mice. However, overall APs in the 24-h recording were significantly higher (Figure 13A, B). The mean AP (MAP) of *Ttn3*$^{-/-}$ mice was significantly higher than that of WT mice (124.4 ± 7.4 vs 103.2 ± 2.9 mmHg, n = 9 and 10, $p < 0.05$, Student t-test) (Figure 13B). The mean heart rate of *Ttn3*$^{-/-}$ mice was also higher than that of WT mice (627.9 ± 11.05 vs 594.1 ± 5.7 bpm, n = 9 and 10, $p < 0.05$, Student t-test) (Figure 13C). More importantly, *Ttn3*$^{-/-}$ mice elicited a larger variation and distribution of MAP than those of

WT mice (Figure 13D and 13E). These parameters are a strong indication of baroreceptor denervation (Cowley et al., 1973). Because the TTN3 is mechanically activated ion channel expressed in nodose ganglia. Knockout of this gene leads to a reduction of baroreceptor sensitivity. Therefore, when blood pressure increases, the baroreceptor fail to transduce signals accordingly, leading to insufficient activation of parasympathetic system. This leads to higher blood pressure in *Ttn3*$^{-/-}$ mice.

6. Ttn3-/- mice shows normal locomotor activity.

In contrast, no significant differences were found in 24h locomotor activity between WT and Ttn3-/- mice (Figure 14A, B).

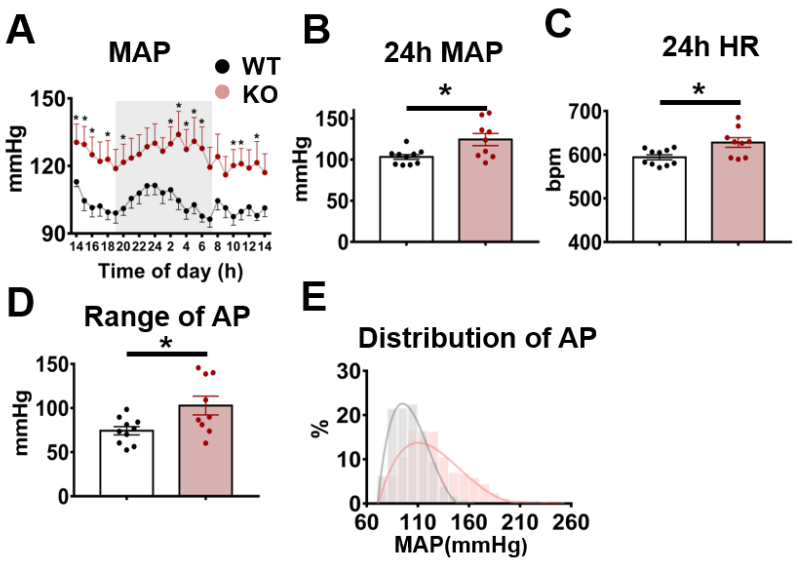

Figure 13. Ttn3 ablation results in hypertension, tachycardia, AP instability, and the reduction in baroreflex sensitivity

(A) Continuous recordings of mean AP (MAP) in WT (n = 10) and Ttn3-/- mice (n = 9) for 24 h. A telemetric device was embedded prior to recording ambient AP in freely moving mice. Readings were made in every hour. Shaded area represents night-time. (* $p < 0.05$, Student's t test)

(B, C) Summarized data of average MAPs and heart rates in 24 h of both genotypes. (* $p < 0.05$, NS; not significant, Student's t test)

(D) Range of AP fluctuations in 24 h in WT and Ttn3-/- mice

(E) Frequency distribution histogram of MAP in 24-hour period in WT (black, n = 10) and Ttn3-/- mice (red, n = 9). (* $p < 0.05$, Student's t-test).

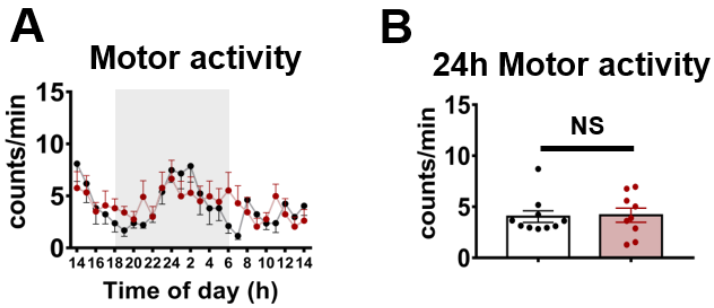

Figure 14. Ttn3-/- mice shows normal locomotor activity

(A) Continuous recordings of mean locomotive activity in WT (n = 10) and Ttn3-/- mice (n = 9) for 24 h. A telemetric device was embedded prior to recording ambient AP in freely-moving mice. Readings were made in every hour. Shaded area represents night time. (* $p < 0.05$, Student's t test)

(B) Summarized data of average motor activities in 24 h of both genotypes. (* $p < 0.05$, NS; not significant, Student's t test)

7. Ttn3-/- mice shows normal respiratory function.

We compared respiratory functions of WT and Ttn3-/- mice using whole-body plethysmography. Respiratory rate, inspiration and expiration time, and tidal volume were assessed. No significant difference was observed among the two groups of mice, showing that Ttn3-/- mice had intact pulmonary functions (Figure 15).

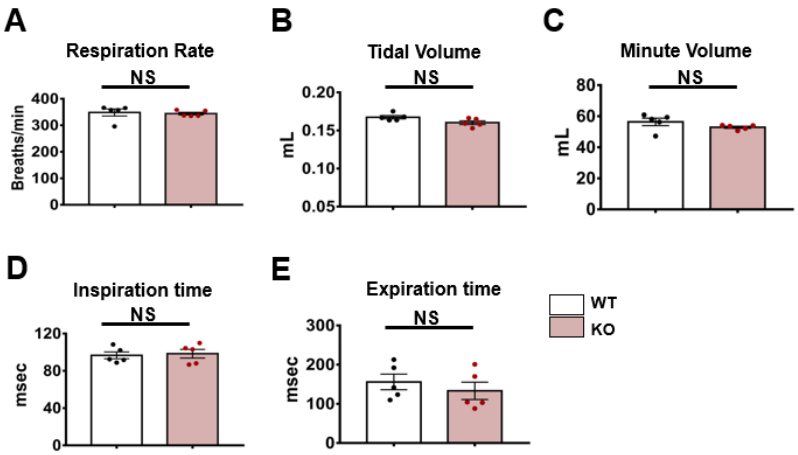

Figure 15. Ttn3-/- mice shows normal pulmonary function
(A) Respiratory rate, (B) tidal volume, (C) Minute Volume, (D) Inspiration time. (E) Expiration time.

8. *Ttn3* ablation impairs baroreflex sensitivity.

We next tested whether genetic deletion of *Ttn3* can lead to changes in baroreflex sensitivity *in vivo*. The gain of baroreflex sensitivity was estimated with the change in HR divided by the changes in systolic pressure (ΔHR/ΔSBP) (Lu et al., 2009; Voss et al., 2000). Bolus injection of phenylephrine (4 μg/Kg), an alpha-adrenergic receptor agonist, to the femoral vein of WT mice increased AP rapidly with a concomitant reflex decrease in the HR (Figure 16A, B). The average increase in systolic blood pressure of *Ttn3*$^{-/-}$ mice after the phenylephrine injection was comparable to that of the WT mice (45.41 ± 5.13 vs 40.37± 7.75 mmHg, n = 7, p = 0.13, Student t-test) (Figure 16C). However, the reflex decrease in the HR in *Ttn3*$^{-/-}$ mice was significantly lower than that of the WT mice (196.2 ± 17.1 vs 118.4 ± 25.5 bpm, $p < 0.05$, Student t-test) (Figure 16D). Therefore, the baroreflex sensitivity of the *Ttn3*$^{-/-}$ mice was significantly less than that of the WT mice ($p < 0.01$, Student t-test) (Figure 16E). Collectively, together with ambient AP and HR changes in *Ttn3*$^{-/-}$ mice, these results clearly indicate

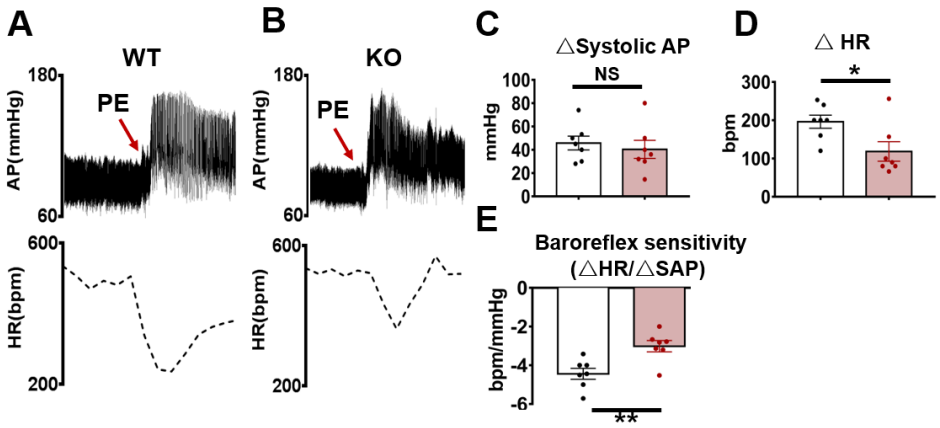

Figure 16. Ttn3 ablation results in the reduction in baroreflex sensitivity

(A, B) Representative tracings showing the changes in AP and HR in response to the intravenous injection of phenylephrine (PE) in conscious WT and Ttn3-/- mice .

(C, D) Average changes in systolic blood pressure (ΔSBP) and heart rate (ΔHR) in response to the intravenous injection of PE in WT and Ttn3-/- mice (* $p < 0.05$, Student's t-test).

(E) Baroreflex sensitivity (ΔHR/ΔSBP) after the intravenous PE injection in WT and Ttn3-/- mice (** $p < 0.01$, Student's t-test).

the active role of TTN3 in mediating the baroreflex *in vivo*.

9. Overexpression of TTN3 in NG of *Ttn3*$^{-/-}$ mice rescues the impaired baroreceptor in *Ttn3*$^{-/-}$ mice

In order to confirm the role of TTN3 in the baroreceptor function, we overexpressed *Ttn3* in NG in *Ttn3*$^{-/-}$ mice to see if the impaired function of baroreceptor is rescued. We injected AAV containing either mCherry (AAV-hsyn-mCherry, control KO group) or *Ttn3*-mCherry gene (AAV-hsyn-*Ttn3*-mCherry, rescue group) into NG of *Ttn3*$^{-/-}$ mice. Robust expression of mCherry was observed with high efficiency in both AAV-hsyn-mCherry and AAV-hsyn-*Ttn3*-mCherry infected NG (72.4 ± 3.6% vs 68.7 ± 5.1%, respectively) of *Ttn3*$^{-/-}$ mice (Figure 15A, B). With the telemetry device, APs and HRs of mice of the control KO and rescue groups were recorded for 24 hours. As shown in Figure 17C-E, the control KO group elicited significant increases in the 24h MAP, HR, and range of APs compared to those of the WT mice. In contrast, the rescue group elicited a significant reduction in the MAP, HR, and range of AP to the levels of the WT mice (Figure 17C-E). In

addition, the rescue group regained the baroreflex sensitivity from that of the control group to the level of the WT group (Figure 17F). These results clearly confirm that TTN3 plays an essential role in the baroreceptor function.

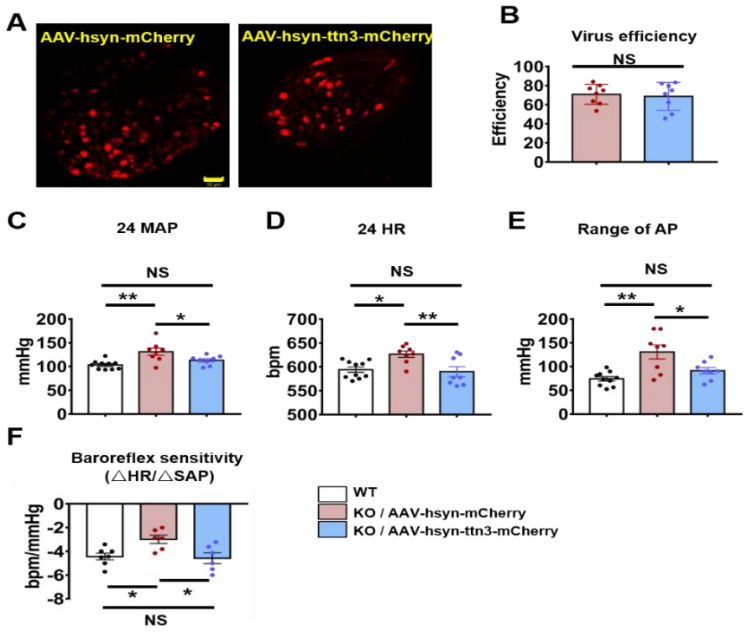

Figure 17. The overexpression of Ttn3 in NG neurons of Ttn3-/- mice rescues the loss of baroreceptor function in Ttn3-/- .

(A) mCherry expression in nodose ganglia of Ttn3-/- mice infected with either AAV-hsyn-mCherry (left) or AAV-hsyn-Ttn3-mCherry (right). Scale bar; 50 μm.

(B) The infection efficiency (% of total cells) of AAV-hsyn-mCherry (n = 1,025 cells) and AAV-hsyn-Ttn3-mCherry (n = 1,161 cells) infected to nodose ganglia of Ttn3-/- mouse.

(C-F) MAP (C), heart rate (D), range of AP (E), and baroreflex sensitivity (F) recorded in 24 h of WT and Ttn3-/- mice infected with either AAV-hsyn-mCherry or AAV-hsyn-Ttn3-mCherry (* $p < 0.05$, ** $p < 0.01$, One-way ANOVA with Tukey's post-hoc test).

10. Chemogenetic inhibition or stimulation of TTN3^{+} neurons in NG induces hypertension or hypotension, respectively

We next investigated whether selective inhibition or activation of TTN3^{+} neurons in NG can affect the baroreflex *in vivo*. We used the designer receptor exclusively activated by designer drug (DREADD) system to test our hypothesis. We injected *AAV-hsyn-DIO-mCherry, AAV-hsyn-DIO-hM4Di-mCherry* or *AAV-hsyn-DIO-hM3Dq-mCherry* into NG of the *Ttn3*^{Cre} mice. These viruses insure mCherry, hM4Di or hM3Dq expression only in *Cre*-expressing NG neurons. hM4Di or hM3Dq are artificially-designed G-protein coupled receptors that stimulate Gi- or Gq-proteins, respectively, to induce inhibition or excitation of neurons upon clozapine-N-oxide (CNO) application (Gomez et al., 2017; Wess et al., 2013). In freely-moving mice with a telemetric pressure probe, the intraperitoneal injection of CNO to the mice infected with *AAV-hsyn-DIO-hM4Di-mCherry* induced a significant increase in MAP and HR (11.9 ± 1.7 vs 0.6 ± 2.7 mmHg, n = 6, $p < 0.01$, 48.7 ± 15.1 vs 6.7 ± 4.8 bpm, n = 6, $p < 0.05$, Student t-test) measured for 10

min, 20 min after the injection (Figure 18A-D) compared to those of mice infected with *AAV-hsyn-DIO-mCherry*. Conversely, the CNO injection to the mice infected with *AAV-hsyn-DIO-hM3Dq-mCherry* induced a significant decrease in MAP and HR (-14.7 ± 1.07 vs 0.6 ± 2.7 mmHg, n = 6, $p < 0.01$, -40.1 ± 7.8 vs 6.7 ± 4.8 bpm, n = 6, $p < 0.01$, Student t-test) (Figure 18A-D). These results further suggest that TTN3-positive NG neurons contribute to the baroreflex function.

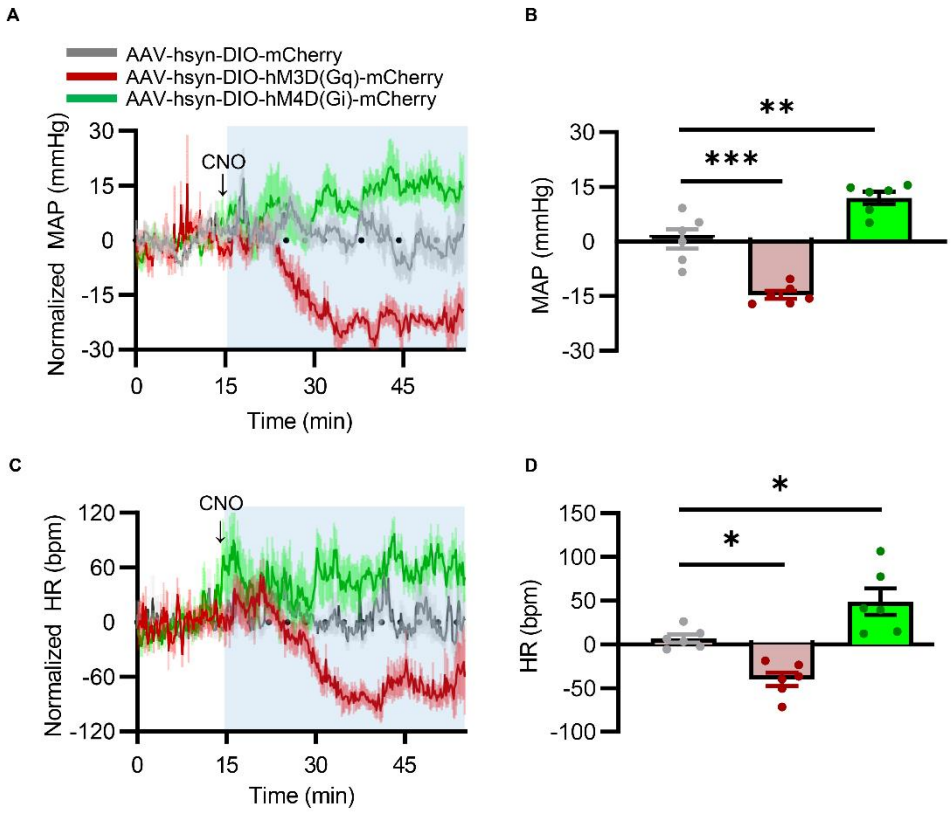

Figure 18. The Chemical Inhibition or activation of TTN3+ neurons in nodose ganglion in vivo

(A and C) MAP(A) and HR(C) responses to CNO injection; data are mean±SEM; Data is normalized to 0 to 15min(baseline, before CNO injection) .

(B and D) Summaries of ΔMAP (B) and Δheart rate (D) responses to CNO injection. (* $p < 0.05$, *** $p < 0.001$, Students t-test).

11. ANO8 was localized in plasma membrane

Mouse Ano8 tagged with enhanced green fluorescence protein (eGFP) was overexpressed in HEK 293T cells. ANO8 was well expressed in the membrane as the eGFP was localized in the plasma membrane with F-actin (Filamentous) (Figure 19).

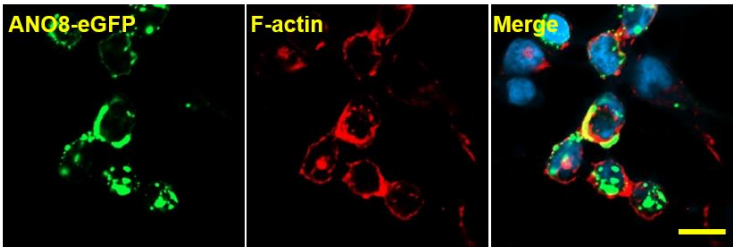

Figure 19. Ano8 was localized in plasma membrane.

(A) The image of overexpression of mAno8-pEGFP-N1 in the HEK293T cells with Hoechst 33342 and f-actin staining. Scale bar represents 50 μm.

12. Ano8 is activated by intracellular cAMP

I tested other stimuli including mechanical, cold , heat, Ca2+, but they all failed to activate ANO8. Among various maneuvers applied to HEK cells transfected with Ano8 (ANO8/HEK cells) in whole cell configuration, robust inward currents were observed only when 100 uM cAMP was added to the intracellular pipette. The pipette (intracellular) solution contained 140 mM KCl. The membrane potential was held at -60 mV (Figure 20A, B). These currents were not observed in HEK293T cells expressing empty vector. The cAMP-induced currents in Ano8-transfected HEK cells would be due to the activity of protein kinase A (PKA), a cAMP-dependent kinase. A PKA inhibitor, H-89(Herbst et al., 2009)was pre-treated before forming whole cells. Indeed, the cAMP-evoked currents were remarkably reduced by the treatment of cells with H-89. However, an Ano1 blocker, MONNA(Oh et al., 2013), failed to inhibit the cAMP-induced currents (Figure 20A, B).

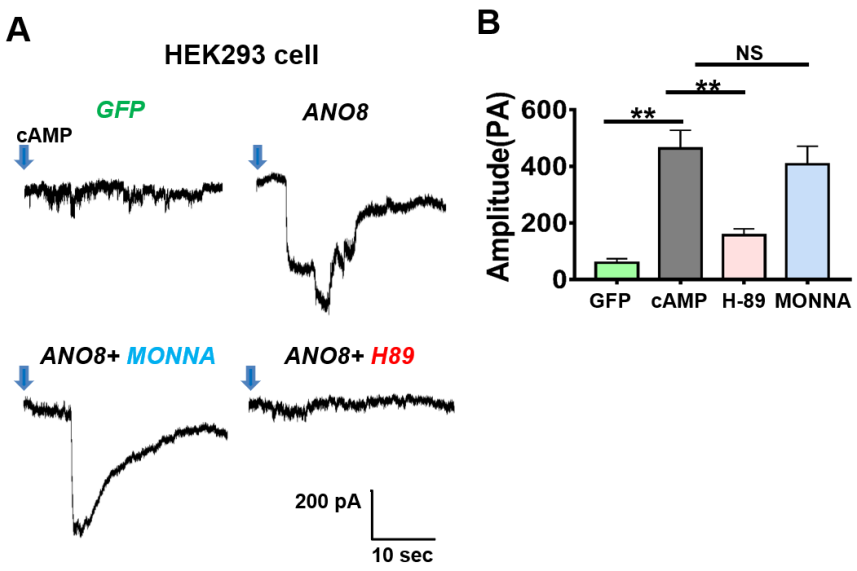

Figure 20. Ano8 was activated by intracellular cAMP.

(A) Representative traces of whole-cell currents in HEK cells transfected with GPF and Ano8.(up left and right). And Ano8 overexpression cells treatment with MONNA, Ano1 antagonist, and H89 (below left and right). The pipette solution contained (mM) 140 KCl, 2MgCl2, 2ATP, 0.3GTP, 10mM HEPES and cAMP(100μM).

(B) Summary of the cAMP-induced whole -cell currents in GFP and ANO8-HEK cells and H89, MONNA pre-treated ANO8 transfected HEK cells. (** $p < 0.01$, One-way ANOVA with Tukey's post-hoc test).

13. Ano8 is a cation channel and not sensitive to voltage

To determine if ANO8 is a cation or anion channel, the 140 mM NaCl bath (extracellular) solution was replaced with N-methyl D-glutamine (NMDG)-Cl solution. The pipette contained 140 mM KCl. The cAMP-evoked currents in ANO8/HEK cells were cationic because the cAMP-induced currents were observed only when the bath solution was 140 mM NaCl solution but not when the bath solution was 140 mM NMDG-Cl solution (Figure 21A, B).

Ano1 is activated weakly by depolarization so that the depolarization synergize the Ca2+-induced ANO1 currents(Yu et al., 2014). Therefore, we also determined whether voltage alone can activate ANO8. The voltage steps from -120 to +120 mV in 10 mV increment were applied to control and *Ano8*-transfected HEK cells (Figure 21C). To block voltage-gated potassium channels in HEK cells, the cells were treated with potassium channel blocker, 4-aminopyridine (Choquet and Korn, 1992). The I-V curves of *Ano*8-expressing HEK cells followed ohmic response, which was similar to those of the control HEK cells (Figure 21D).

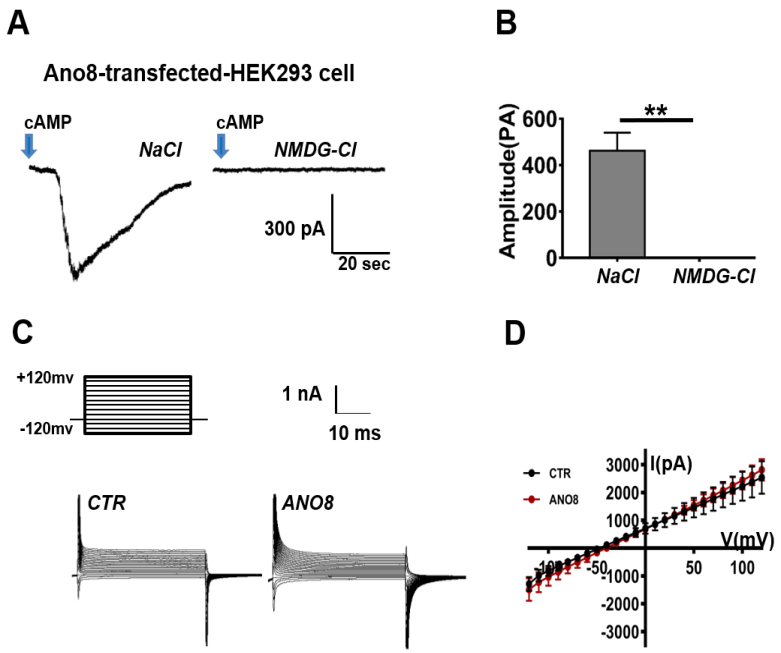

Figure 21. Ano8 is cation channel and not sensitive to voltage

(A) The cAMP induced whole-cell currents were observed in NaCl (left) but not in NMDG-Cl (right) bath solution.

(B) Summary of the cAMP-induced whole -cell currents of ANO8-HEK cells in NaCl and NMDG-Cl bath solution.

(C) Representative traces of whole currents of ANO8 transfected HEK cells or GFP transfected HEK cells. activated by voltage. Voltage steps from -120 mv to +120mv in 10 mv increments.

(D) I-V curves of ANO8-HEK cells activated by voltage. (* $p < 0.05$, Student's t test).

14. Intracellular Calcium enhances cAMP-induced currents of Ano8

Since ANO1 and ANO2 are activated by intracellular Ca2+ and voltage. Furthermore, Calcium-activated and apoptotic phospholipid scrambling induced by Ano6. So, we wonder whether intracellular calcium also can activate Ano8 as well. Various concentrations of intracellular calcium added to the pipette solutions (Fig. 22A). 1uM Ca^{2+}, 30uM cAMP or 10uM Ca^{2+} alone can hardly evoke any currents from Ano8-overexpression HEK cells (27.51 ± 9.23 pA, 45.00 ± 15.28 pA, 90.83 ± 27.41 pA n = 6.) However, when 30 uM cAMP was applied together with 1uM Ca^{2+}, whole cell current was observed (428.20 ± 51.98 pA, n = 5). In addition, when 30 uM cAMP was applied together with 10uM Ca^{2+}, significantly currents was observed, and the amplitude (949.84 ± 99.45 pA, n = 5) was larger than those activated by 1uM Ca^{2+} together with 30 uM cAMP (Fig. 22A.B). those results showed that with intracellular calcium, cAMP-induced currents were largely enhanced in Ano8-overexpression HEK cells.

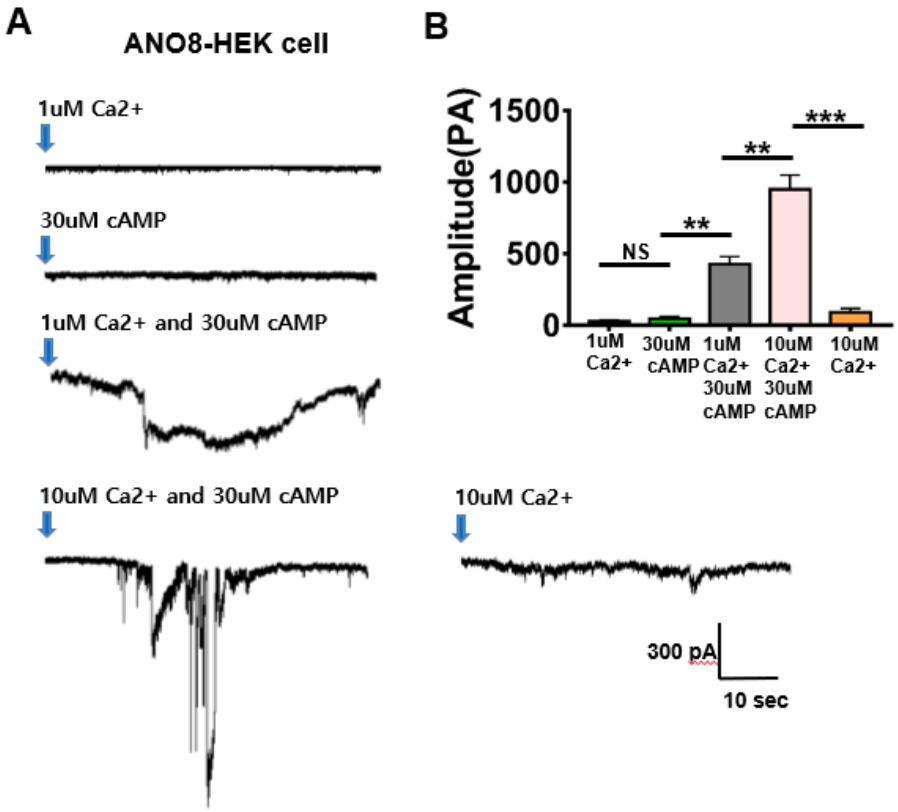

Figure 22. Intracellular calcium amplifies cAMP-evoked currents of ANO8

(A) Representative traces of cAMP activated currents in ANO8-HEK cells with different concentrations of Ca^{2+}.

(B) Summary of the cAMP-induced whole -cell currents of ANO8-HEK cells in 1 or 10um Ca^{2+}. (* $p < 0.05$, ** $p < 0.01$, One-way ANOVA with Tukey's post-hoc test, Student's t test).

15. ANO8 is highly expressed in cortex, brainstem, cerebellum, spinal cord and dorsal-root ganglia.

In order to determine the tissue distribution of ANO8, we checked transcripts of *Ano8* by RT-PCR analysis and immunostaining in sixteen mouse tissue samples (Figure 23A). *Ano8* transcripts were high in the nervous system including cortex, brainstem, cerebellum, spinal cord and dorsal-root ganglia (Figure 23A and Figure 24). The presence of *Ano8* transcripts in dorsal-root ganglion (DRG) was also confirmed in PCR analysis (Figure 23B). The RT-PCR analysis of DRG neurons further revealed the *Ano8* expression as high as *Trpv1*, a representative channel for nociception (Basbaum et al., 2009; Caterina et al., 1997; Tominaga et al., 1998). In addition, its transcript level exceeded that of Ano1, which is also known to be present in DRG with nociceptive function (Cho et al., 2012; Lee et al., 2014).

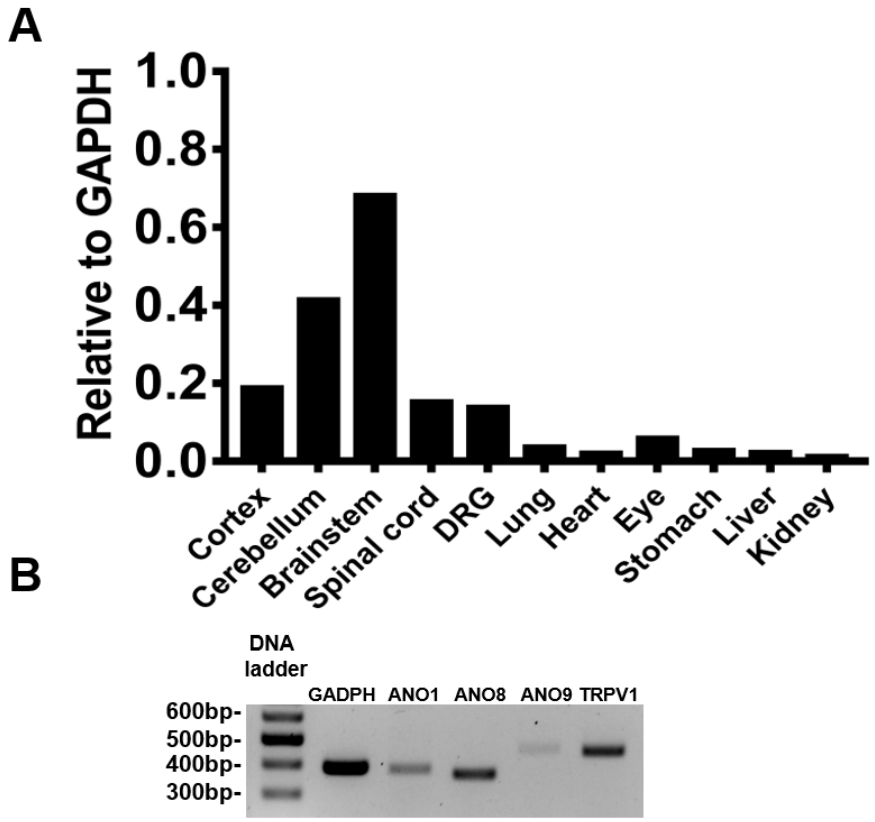

Figure 23. ANO8 is highly expressed in cortex, brainstem, cerebellum, spinal cord and dorsal-root ganglia.

(A) mRNA transcript levels of ANO8 in various mouse tissue organs. Note that ANO8 is highly expressed central nerve system and DRGs.

(B) The mRNA expression of ANO8 in DRG neurons assayed by RT-PCR.

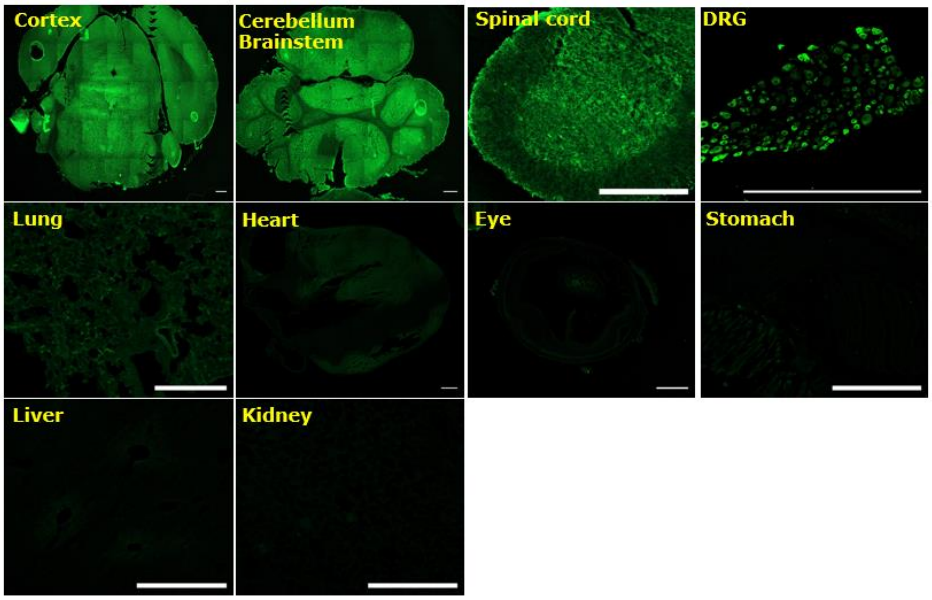

Figure 24. Immunostaining confirm ANO8 expression

ANO8 immunostaining expression in various mouse tissue organs. Note that ANO8 is highly expressed central nerve system and DRGs. Scale bar represents 500 μm.

16. ANO8 antibody specific confirm.

To confirm the antibodies specificity, we transfected empty vector (GFP), TTN3 or ANO8 gene into HEK cells, then perform immunostaining on these cells. The antibodies only stain TTN3- or ANO8-positive cells, not the non-transfected cells or those transfected with empty vector. This shows that the antibodies are specific. (Figure 25).

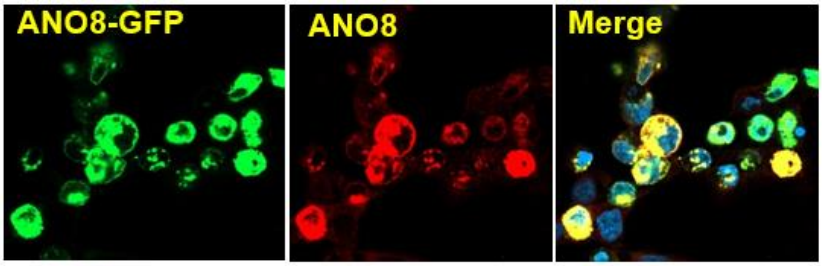

Figure 25. ANO8 antibody was co-expressed with ANO8 gene.

17. ANO8 is highly expressed in nociceptive neurons

To determine its physiological role in somatosensory functions, Ano8-expressing cell type was assayed in DRG neurons with ANO8 antibody. Thin sections of DRGs were stained with the *Ano8* antibody together with neurofilament H (NFH), a marker for myelinated axons, CGRP, a marker for peptidergic small sensory neurons, TRPV1, nociceptor marker and isolectin B4 (IB4), a marker of non-peptidergic small sensory neurons. Shown in Figure 26A, ANO8-immunofluorescence was present in DRG neurons. ANO8 appeared to be expressed in a subset of small-diameter DRG neurons because ANO8 immunoreactivity was observed in small portions (27.56%) of neurofilament H, a marker for myelinated neurons. Consistent with this, (43.92%) of ANO8-positive DRG neurons were colocalized with TRPV1. Among nociceptors, a greater portion (56.76%) of ANO8-positive neurons were positive with isolectin B4 than CGRP (30.04%), suggesting that ANO8 is largely expressed in the non-peptidergic nociceptive DRG neurons.

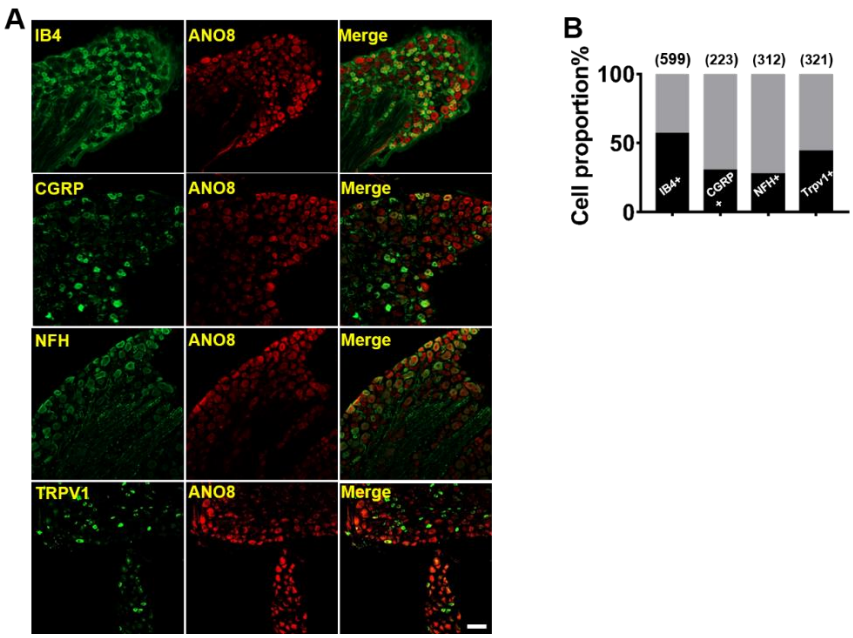

Figure 26. ANO8 is highly expressed in nociceptive neurons.

(A) Immunofluorescent images of ANO8 in DRGs. The DRG neurons were stained with IB4, CGRP, neurofilament H (NFH) and TRPV1. Scale bar represents 50 μm.

(B) Proportion of IB4+, CGRP+, NFH+ and TRPV1+ neurons among ANO8+ DRG neurons.

18. ANO8 confers cAMP-dependent channel currents in DRG

We then wondered whether intracellular cAMP can activate endogenous Ano8 in DRG neurons. Whole-cell currents were recorded from relatively small-sized DRG neurons (diameter < 20 um). As shown Figure 27A, the intracellular application of 100 uM cAMP evoked inward currents with amplitude of 192.93 ± 19.52 pA (n = 6). In contrast, the konck-down by transfection with *Ano8* siRNA significantly reduced the cAMP-induced currents (114.62 ± 14.10 pA, n = 5) (Figure 27A, B). These results demonstrate that endogenous ANO8 in DRG neurons is functionally activated by intracellular cAMP.

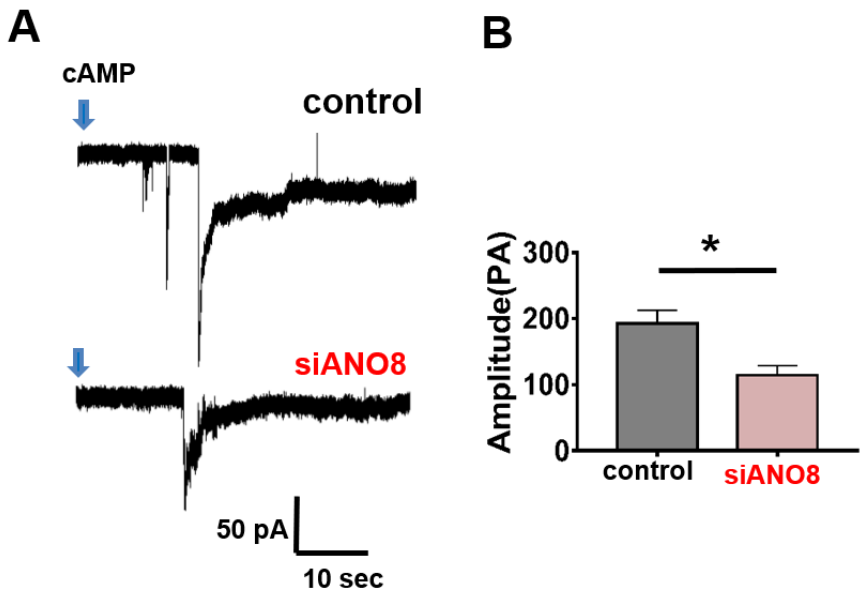

Figure 27. ANO8 functions as a cAMP-activated channel in DRG

(A) Representative traces of cAMP induced whole currents of scr treatment or siANO8 treatment DRG neurons.

(B) The average current amplitude of scr treatment or siANO8 treatment DRG neurons activated by intracellular cAMP. (* $p < 0.05$, Student's t test).

19.ANO8 mediates Pain sensitivity in acute nociceptive pain model

Because of the high expression of ANO8 in DRG neurons, we expected the possible role of ANO8 in nociception. Therefore, we designed *AAV-CMV-mCherry-Ano8-shRNA* virus *and AAV-CMV-mCherry* virus for control and injected into L4-L5 DRGs to knock down *Ano8* (Figure 28A, B). After four weeks recovery, a nociceptive behavioral test was performed. Intraplantar formalin injection used for the nociceptive behavioral test because the formalin test is a reliable and widely used pain model (Abbott et al., 1995)(Figure 28C). The typical nociceptive response to the formalin injection is biphasic, which consists the early transient response lasting for the first 10 min and the late phase from 10 to 60 min (Abbott et al., 1995). Naïve mice without the viral infection (wild-type group) and mice infected with AAV-control showed the typical biphasic licking responses after the formalin injection (Figure 28D, E). In contrast, mice infected with *AAV-CMV-mCherry-Ano8-shRNA* virus showed significantly less licking

behavior during the second phase, but not in the first phase, compared to those of WT and AAV-control group mice(Second phase:260.0±9.3s vs 357.5±23.6s, $p < 0.01$, First phase: 105.0±5.5 vs 92.3±10.1s, $p > 0.05$, AAV-shRNA group VS AAV-control)(Figure 28D, E).

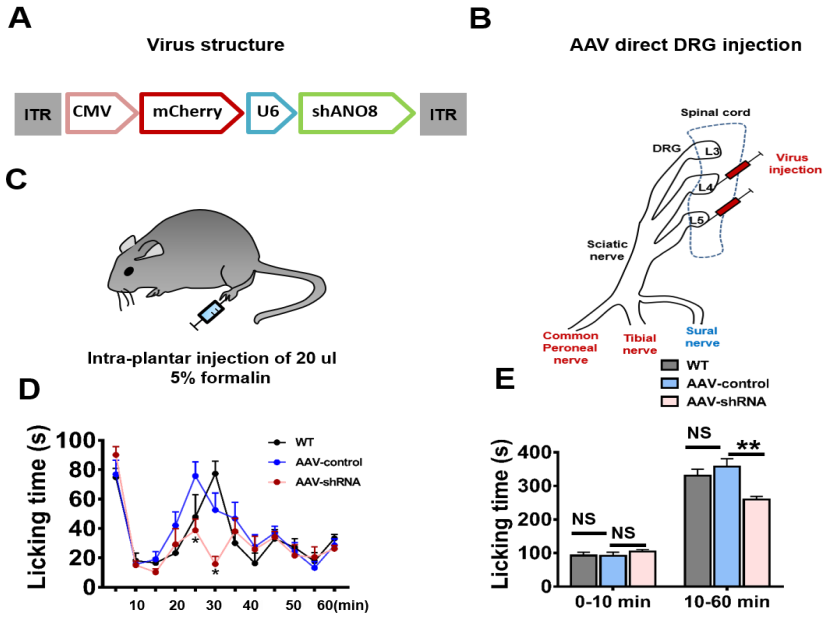

Figure 28. Decrease pain sensitivity after intraplate injection of formalin in DRG (L4-L5) ANO8 Knock-down mice

(A) Targeting strategy for deleting ANO8 mRNA. The mouse U6 promoter was used to drive the expression of ANO8-shRNA.

(B) Schematic diagram showing injection of virus into L4-L5(DRG).

(C) Schematic diagram of the formalin pain models.

(D) Licking duration of hindpaw at 5-min intervals for 1 h in the formalin pain model of WT, control virus and ANO8-shRNA virus goup.

(E) Quantification of the formalin response binned into different phases. (* $p < 0.05$, ** $p < 0.01$, One-way ANOVA with Tukey's posthoc test).

20. Ano8 knock-down reduces the activities of dorsal-horn neurons

c-Fos is the protein encoded by the proto-oncogene *c-fos* and has been extensively used as a marker for neuronal activity in various regions including in the spinal cord (Harris, 1998). We therefore sought to assess the change in neuronal activity of dorsal horn neurons of the L4-L5 spinal cord using c-Fos immunofluorescence technique. After the formalin injection into the left hind paw, c-Fos signals were observed throughout the ipsilateral dorsal horn of the lumbar spinal cord (Figure 29 A). c-Fos positive neurons were densely populated in the superficial lamina of the dorsal horn. The number of c-Fos-positive neurons in the dorsal horn was significantly lower in *AAV-CMV-mCherry-Ano8-shRNA* infected mice (Figure 29A, B). These results suggest that ANO8 participates in nociception.

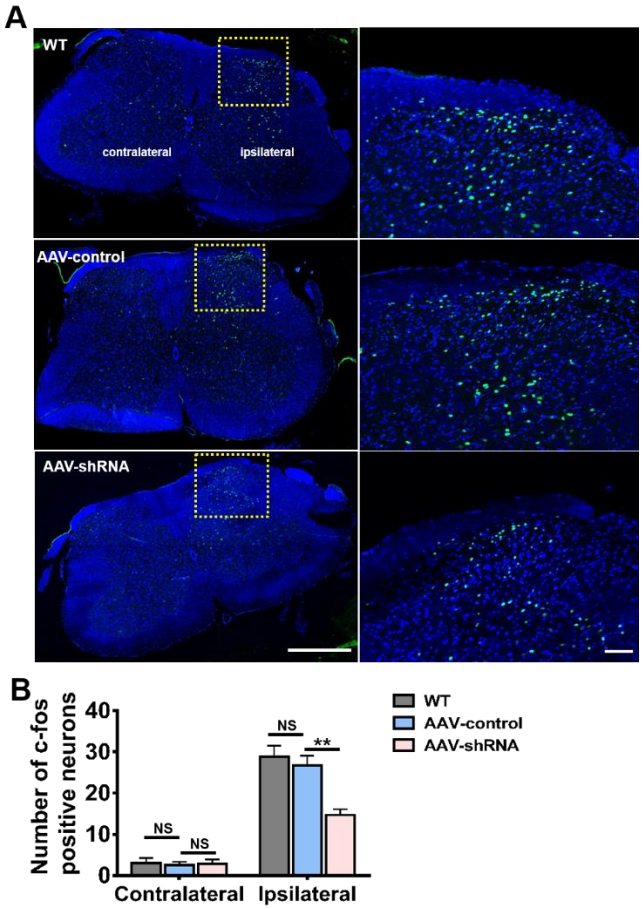

Figure 29. Ano8 knock-down reduces the activities nociceptive dorsal-horn neurons in the spinal cord

(A) c-Fos immunohistochemistry of spinal cord after formalin test. Boxed regions are magnified at right. Scale bars, 500 μm. Con, contralateral; Ip, ipsilateral.

(B) Summary of c-fos positive neurons number counting. (* $p < 0.05$, ** $p < 0.01$, One-way ANOVA with Tukey's posthoc test).

DISCUSSION

1. The role of TMEM150C in baroreceptor function

AP changes rapidly from moment to moment in our daily life. Because high or low blood pressure is detrimental or sometimes lethal, buffering the AP change is important. The baroreflex is one of the control mechanisms that regulate AP in normal life (Fernandez et al., 2015; Victor, 2015). The baroreflex is a powerful and fast neural control mechanism of AP (Hall and Guyton, 2011). It depends on baroreceptor activity in the aortic arch and carotid sinus, which sense AP changes and send neural signals to the cardiovascular center. Sensing pressure changes in the arteries requires the activity of molecular sensors in baroreceptors in the aortic arch or carotid sinus. The present study presents evidence that TTN3, a newly discovered MA channel, functions as a mechanotransduction channel in baroreceptors. (i) Expression of TTN3 in NG neurons as well as in the terminals of ADN innervating in the aortic arch, (ii) absence of SA MA currents in

aorta-projecting NG neurons of *Ttn3*$^{-/-}$ mice, (iii) reduction in basal and pressure-induced ADN activity in *Ttn3*$^{-/-}$ mice, (iv) increased MAP, HR and fluctuation of MAP in *Ttn3*$^{-/-}$ mice, (v) rescue of the impaired baroreceptor function after overexpression of *Ttn3* in NGs of *Ttn3*$^{-/-}$ mice, (vi) chemogenetic stimulation or inhibition of TTN3-expressing neurons in NG lowered or increased MAP and HR, respectively. Because the dysfunction of baroreflex causes fatal diseases, the identification of molecular sensors in baroreceptors can provide a useful clue to treat cardiovascular diseases.

Effects of functional ablation of Ttn3 on baroreceptor function

The denervation of ADN or carotid sinus nerve is known to result in acute hypertension, tachycardia, and larger fluctuation of APs in dogs, rabbits, rodents, and human (Cowley et al., 1973; Faris et al., 1980; Martinka et al., 2005; Thrasher, 2005). The bilateral denervation of carotid sinus leads to chronic hypertension in human and other animals except for dogs whose denervation of aortic baroreceptors only leads to short-term hypertension (Cowley

et al., 1973; Faris et al., 1980; Martinka et al., 2005; Thrasher, 2005). Among the cardiovascular changes, variability in AP after baroreceptor denervation is more consistent. Thus, stabilizing AP appears to be a primary function of baroreceptors. The present study showed a significantly high MAP as well as the variability of AP in *Ttn3*$^{-/-}$ mice compared to WT mice, whose abnormalities were rescued when TTN3 was overexpressed in NG of the *Ttn3*$^{-/-}$ mice.

When the basal baroreceptor input to the central cardiovascular center is withdrawn, the sympathetic outflow will increase while the parasympathetic outflow will decrease, which leads to hypertension and tachycardia (Lau et al., 2016; Lu et al., 2009). In the present study, hypertension and tachycardia were found in *Ttn3*$^{-/-}$ mice. The phenotype of *Ttn3* ablation resulted from the dysfunction in baroreceptor afferents, not in the central cardiovascular center. This assumption is also supported in part by the rescue experiment or chemogenetic modulation of TTN3-positive neurons in NG, because overexpression of *Ttn3*, hM3Dq,

or hM4Di in NG, not in the brain, is sufficient to rescue or modulate the baroreflex.

Roles of Piezo channels and TTN3 in baroreceptors

Surprisingly, the MA currents in aorta-projecting NG neurons are similar to those found in dorsal-root ganglion neurons (Coste et al., 2010; Hong et al., 2016). This is the first time to characterize MA currents in baroreceptor neurons. In response to step mechanical stimuli, three different MA currents such as RA, IA, and SA currents, were observed. In dorsal-root ganglion neurons, SA currents are known to be mediated by TTN3 whereas Piezo2 is responsible for RA currents (Coste et al., 2010; Hong et al., 2016). Consistent with somatosensory neurons, SA MA currents in NG neurons were markedly diminished in *Ttn3*$^{-/-}$ NG neurons. In addition, a large proportion of aorta-projecting NG neurons also elicit RA MA currents. The presence of RA MA currents in NG neurons suggests a role of Piezo 1 or 2 in baroreceptor function. Indeed, Zeng and colleagues reported that Piezo 1 and 2 mediate the baroreceptor function (Zeng et al., 2018).

Piezo 2 are expressed in NG neurons. Piezo 1 and 2 double KO mice show hypertension, tachycardia, and the loss of the baroreceptor sensitivity (Zeng et al., 2018). Piezo 1 and 2 appear essential for sensing AP changes in baroreceptors, which largely overlaps with the functional role of TTN3 in AP sensing in baroreceptors. Perhaps these findings indicate that the redundancy in molecular sensors is required for important physiological functions so that mutations in one type of channels would not affect much to the system. However, TTN3 and Piezo channels may play a different role in sensing AP changes in baroreceptors. Myelinated or unmyelinated fibers in ADN fibers showed different pressure sensitivity and maximal firing rates (Brown, 1980; Brown et al., 1978; Seagard et al., 1990). In addition, the baroreflex gain is higher to sinusoidal pressure changes than steady-state pressure changes (Brown, 1980; Schmidt et al., 1972). Rencently, transcriptomes of single NG neurons were analyzed with single-cell RNA-sequencing technique (Kupari et al., 2019). Based on the unique gene expression patterns, Patrik Ernfors team classified 18

NG neuronal clusters that are consistent with chemo-, baro-, stretch-, and volume-sensor functions of vagal afferents. According to their cell cluster database, *Ttn3* expresses in all 18 NG cell clusters with high expression in NG1-3 and NG12-18, which is in sharp contrast to the expression patterns of Piezo1 and 2 (Kupari et al., 2019). Therefore, the two groups of channels may have distinct roles in sensing phasic or tonic AP with different sensitivity to AP.

Pathology of the baroreflex dysfunction

Baroreflex stabilizes APs. Therefore, when the sensitivity of baroreflex is blunted, many fatal diseases such as hypertension, stroke, and heart failure ensue (Dauphinot et al., 2013; Mostarda et al., 2011; Sykora et al., 2010). The removal of sinoaortic baroreceptor due to trauma or radiation therapy for head and neck cancer causes paroxysmal hypertension or a sharp increase in blood pressure after minor emotional stress (Aksamit et al., 1987; Heusser et al., 2005). Patients with familial dysautonomia display abnormality in baroreceptor afferent input. These patients have elevated supine blood pressure and marked hypertension upon mild

mental stress (Norcliffe-Kaufmann et al., 2010; Riley and Friedman, 1981). In addition, the baroreflex sensitivity slows down with age because of the stiffness of blood vessels in the big arteries, which is one of the causes of hypertension of elderly people (Dauphinot et al., 2013). Now, the AP buffering mechanism of baroreceptors becomes a useful tool to treat chronic cardiovascular diseases. Carotid sinus nerve stimulation is attempted clinically to cure resistant hypertension as well as chronic heart failure (Victor, 2015; Yin and Slavin, 2015). Therefore, understanding the molecular mechanisms underlying the baroreceptor function may be applied to conditions of improving untreatable cardiovascular diseases.

2. The role TMEM16H in Nociceptive function

The Anoctamin gene family is a group of 10 membrane proteins with various physiological as well as pathological functions. Although biophysical and their physiological functions of many Anoctamin genes are now known, whether ANO8 is a channel or not is not known. The present study characterized the biophysical

property of ANO8 as a channel. To our surprise, ANO8 is a cation channel activated by cAMP, which is distinct from ANO1 and ANO2 that are anion channels activated by intracellular Ca2+. The overall expression of ANO8 is high the nervous system including somatosensory ganglia. Moreover, the downregulation of Ano8 in the lumbar DRGs reduced formalin-induced inflammatory pain. Thus, present study defines the molecular as well as physiological functions of ANO8.

Diverse functions of Anoctamin genes

Anoctamin gene family attracted great attention after the identification of ANO1 as a calcium-activated chloride channel (Caputo et al., 2008; Schroeder et al., 2008; Yang et al., 2008a). ANO1 is a multimodal Cl^- channel activated by intracellular Ca^{2+}, voltage, and heat (Cho et al., 2012; Yang et al., 2008a). ANO1 functions include transepithelial fluid secretion in various epithelia, control of smooth muscle tone in blood vessels, tumorigenesis, and prostate enlargement (Cha et al., 2015; Jang and Oh, 2014; Jun et al., 2017; Pedemonte and Galietta, 2014). ANO1 is also expressed

in DRG neurons with nociceptive functions (Cho et al., 2012; Lee et al., 2014). ANO2 is also known to be a Ca2+-activated Cl- channel with olfactory, retinal, and learning and memory functions (Billig et al., 2011; Huang et al., 2012b; Keckeis et al., 2017a; Rasche et al., 2010). ANO3 is also expressed highly in DRG neurons controlling nociception despite its role as a channel (Huang et al., 2013). ANO5 is mainly found in skeletal system. A missense mutation of *Ano5* is associated with gnathodiaphyseal dysplasia, an autosomal dominant inherited bone disorder (Lv et al., 2019; Marconi et al., 2012), and muscular dystrophy or myopathy (Silva et al., 2019). However, the biophysical role of ANO5 as a channel is obscure. More surprising finding in Anoctamin family is that ANO6 is a scramblase that disrupts phospholipids in the membrane (Suzuki et al., 2010; Yu et al., 2015). A mutation of *Ano6* that truncates the ANO6 protein is associated with a rare bleeding disorder, the Scott syndrome (Suzuki et al., 2010; Yang et al., 2012). Recently, ANO9 was identified as a non-selective cation channel activated by cAMP with possible involvement in metastasis of

colorectal cancer (Kim et al., 2018; Li et al., 2015). Here, the present study revealed that ANO8 works as a cation channel in the nociceptive pathway. Thus, Anoctamin gene family has diverse physiological functions in various organs with different molecular properties.

A possible Role of ANO8 in nociception

DRG neurons are heterogeneous in their functions and size. Small-diameter DRG neurons comprise the majority of nociceptors that transmit pain and itch signals. The nociceptors can be further subdivided to peptidergic and non-peptidergic nociceptors, the latter binds the isolectin B4 (IB4) and expresses the *Mrg* gene family. Interestingly, a significant portion of ANO8 positive neurons were co-stained with IB4, suggesting the possible role in nociception. It was well known that nociceptors were equipped with many ion channels, which works as molecular transducer sensors detecting noxious stimuli or as transmission machinery (Oh and Jung, 2016). Among Anoctamins, ANO1 and ANO3 are implicated in nociception. ANO1 mediates thermal pain as a heat

sensor because mice lacking *Ano1* in DRG neurons are significantly insensitive to noxious heat (Cho et al., 2012; Lee et al., 2014). ANO3 (TMEM16C) appears to contribute to nociception. In contrast, ANO3 is known to induce hypersensitivity in nociception by controlling the expression of Slack channels (Huang et al., 2013). Numerous studies demonstrated the involvement of the cAMP-PKopA pathway in inflammatory, neuropathic, and bone cancer pain (Huang et al., 2012c; Lewin and Walters, 1999; Malmberg et al., 1997; Zhu et al., 2016). For example, the inhibition of adenylyl cyclase (AC) or PKA activity prevents chronic pain including neuropathic pain (Kim et al., 2007; Song et al., 2006). Because ANO8 is a nonselective cation channel expressing in nociceptors, thus ANO8 likely contributes to the cAMP-PKA-dependent nociception. Indeed, the *Ano*8-downregulatoin led to the reduction in nociceptive behaviors in the present study.

REFERENCES

Abbott, F.V., Franklin, K.B., and Westbrook, R.F. (1995). The formalin test: scoring properties of the first and second phases of the pain response in rats. Pain *60*, 91-102.

Aksamit, T.R., Floras, J.S., Victor, R.G., and Aylward, P.E. (1987). Paroxysmal hypertension due to sinoaortic baroreceptor denervation in humans. Hypertension *9*, 309-314.

Aley, K.O., and Levine, J.D. (1999). Role of protein kinase A in the maintenance of inflammatory pain. Journal of neuroscience *19*, 2181-2186.

Askwith, C.C., Wemmie, J.A., Price, M.P., Rokhlina, T., and Welsh, M.J. (2004). Acid-sensing ion channel 2 (ASIC2) modulates ASIC1 H+-activated currents in hippocampal neurons. Journal of biological chemistry *279*, 18296-18305.

Basbaum, A.I., Bautista, D.M., Scherrer, G., and Julius, D. (2009). Cellular and molecular mechanisms of pain. Cell *139*, 267-284.

Bautista, D.M., Siemens, J., Glazer, J.M., Tsuruda, P.R., Basbaum, A.I., Stucky, C.L., Jordt, S.E., and Julius, D. (2007). The menthol receptor TRPM8 is the principal detector of environmental cold. Nature *448*, 204-208.

Biel, M. (2009). Cyclic nucleotide-regulated cation channels. The Journal of biological chemistry *284*, 9017-9021.

Billig, G.M., Pal, B., Fidzinski, P., and Jentsch, T.J. (2011). Ca2+-activated Cl- currents are dispensable for olfaction. Nature neuroscience *14*, 763-769.

Bounoutas, A., and Chalfie, M. (2007). Touch sensitivity in Caenorhabditis elegans. Pflugers Archiv : European journal of physiology *454*, 691-702.

Braga, V.A., Burmeister, M.A., Sharma, R.V., and Davisson, R.L. (2008). Cardiovascular responses to peripheral chemoreflex activation and comparison of different methods to evaluate baroreflex gain in conscious mice using telemetry. American journal of physiology Regulatory, integrative and comparative physiology *295*, R1168-1174.

Brierley, S.M., Hughes, P., Harrington, A., and Ashley Blackshaw, L. (2012). Chapter 24 - Innervation of the Gastrointestinal Tract by Spinal and Vagal Afferent Nerves. In Physiology of the Gastrointestinal Tract (Fifth Edition), L.R. Johnson, F.K. Ghishan, J.D. Kaunitz, J.L. Merchant, H.M. Said, and J.D. Wood, eds. (Boston: Academic Press), pp. 703-731.

Brown, A.M. (1980). Receptors under pressure. An update on baroreceptors. Circulation research *46*, 1.

Brown, A.M., Saum, W.R., and Yasui, S. (1978). Baroreceptor dynamics and their relationship to afferent fiber type and hypertension. Circulation research *42*, 694-702.

Butz, G.M., and Davisson, R.L. (2001). Long-term telemetric measurement of cardiovascular parameters in awake mice: a physiological genomics tool. Physiological genomics *5*, 89-97.

Caputo, A., Caci, E., Ferrera, L., Pedemonte, N., Barsanti, C., Sondo, E., Pfeffer, U., Ravazzolo, R., Zegarra-Moran, O., and Galietta, L.J. (2008). TMEM16A, a membrane protein associated with calcium-dependent chloride channel activity. Science *322*, 590-594.

Carles, A., Millon, R., Cromer, A.,Lemaire, F., Young, J., Wasylyk, C., Muller, D., Schultz, I., Rabouel, Y.*, et al.* (2006). Head and neck squamous cell carcinoma transcriptome analysis by comprehensive validated differential display. Oncogene *25*, 1821-1831.

Carr, M.J., and Undem, B.J. (2003). Bronchopulmonary afferent nerves. Respirology *8*, 291-301.

Catalan, M.A., Kondo, Y., Pena-Munzenmayer, G., Jaramillo, Y., Liu, F., Choi, S., Crandall, E., Borok, Z., Flodby, P., Shull, G.E.*, et al.* (2015). A fluid secretion pathway unmasked by acinar-specific Tmem16A gene ablation in the adult mouse salivary gland. Proceedings of the National Academy of Sciences of the United States of America *112*, 2263-2268.

Caterina, M.J., Leffler, A., Malmberg, A.B., Martin, W.J., Trafton, J., Petersen-Zeitz, K.R., Koltzenburg, M., Basbaum, A.I., and Julius, D. (2000). Impaired nociception and pain sensation in mice lacking the capsaicin receptor. Science (New York, NY) *288*, 306-313.

Caterina, M.J., Rosen, T.A., Tominaga, M., Brake, A.J., and Julius, D. (1999). A capsaicin-receptor homologue with a high threshold for noxious heat. Nature *398*, 436-441.

Caterina, M.J., Schumacher, M.A., Tominaga, M., Rosen, T.A., Levine, J.D., and Julius, D. (1997). The capsaicin receptor: a heat-activated ion channel in the pain pathway. Nature *389*, 816-824.

Catterall, W.A. (2011). Voltage-gated calcium channels. Cold Spring Harbor perspectives in biology *3*, a003947.

Cha, J.Y., Wee, J., Jung, J., Jang, Y., Lee, B., Hong, G.S., Chang, B.C., Choi, Y.L., Shin, Y.K., Min, H.Y.*, et al.* (2015). Anoctamin 1 (TMEM16A) is essential for testosterone-induced prostate hyperplasia. PNAS *112*, 9722-9727.

Cho, H., Yang, Y.D., Lee, J., Lee, B., Kim, T., Jang, Y., Back, S.K., Na, H.S., Harfe, B.D., Wang, F.*, et al.* (2012). The calcium-activated chloride channel anoctamin 1 acts as a heat sensor in nociceptive neurons. Nature neuroscience *15*, 1015-1021.

Choquet, D., and Korn, H. (1992). Mechanism of 4-aminopyridine action on voltage-gated potassium channels in lymphocytes. The Journal of general physiology *99*, 217-240.

Christensen, O., and Zeuthen, T. (1987). Maxi K+ channels in leaky epithelia are regulated by intracellular Ca2+, pH and membrane potential. Pflugers Arch *408*, 249-259.

Coscoy, S., and Barbry, P. (2004). The ENaC/Deg family of cation channels. In Advances in Molecular and Cell Biology (Elsevier), pp. 303-329.

Coste, B., Mathur, J., Schmidt, M., Earley, T.J., Ranade, S., Petrus, M.J., Dubin, A.E., and Patapoutian, A. (2010). Piezo1 and Piezo2 are essential components of distinct mechanically activated cation channels. Science (New York, NY) *330*, 55-60.

Cowley, A.W., Jr., Liard, J.F., and Guyton, A.C. (1973). Role of baroreceptor reflex in daily control of arterial blood pressure and other variables in dogs. Circulation research *32*, 564-576.

Dauphinot, V., Kossovsky, M.P., Gueyffier, F., Pichot, V., Gosse, P., Roche, F., and Barthelemy, J.C. (2013). Impaired baroreflex sensitivity and the risks of new-onset ambulatory hypertension, in an elderly population-based study. Int J Cardiol *168*, 4010-4014.

Doan, T.N., Stephans, K., Ramirez, A.N., Glazebrook, P.A., Andresen, M.C., and Kunze, D.L. (2004). Differential distribution and function of hyperpolarization-activated channels in sensory neurons and mechanosensitive fibers. J Neurosci *24*, 3335-3343.

Donoghue, S., Garcia, M., Jordan, D., and Spyer, K.M. (1982). Identification and brain-stem projections of aortic baroreceptor afferent neurones in nodose ganglia of cats and rabbits. J Physiol *322*, 337-352.

Drummond, H.A., Price, M.P., Welsh, M.J., and Abboud, F.M. (1998). A molecular component of the arterial baroreceptor mechanotransducer. Neuron *21*, 1435-1441.

Dubin, A.E., Murthy, S., Lewis, A.H., Brosse, L., Cahalan, S.M., Grandl, J., Coste, B., and Patapoutian, A. (2017). Endogenous Piezo1 Can Confound Mechanically Activated Channel Identification and Characterization. Neuron *94*, 266-270 e263.

Duran, C., and Hartzell, H.C. (2011). Physiological roles and diseases of Tmem16/Anoctamin proteins: are they all chloride channels? Acta pharmacologica Sinica *32*, 685-692.

Faris, I.B., Iannos, J., Jamieson, G.G., and Ludbrook, J. (1980). The carotid sinus baroreceptor reflex in conscious rabbits. J Physiol *298*, 321-331.

Fernandez, G., Lee, J.A., Liu, L.C., Gassler, J.P., Iliescu, R., Tudorancea, I., and Lohmeier, T.E. (2015). The Baroreflex in Hypertension

Baroreflex activation: from mechanisms to therapy for cardiovascular disease. Curr Hypertens Rep *17*, 19.

Gomez, J.L., Bonaventura, J., Lesniak, W., Mathews, W.B., Sysa-Shah, P., Rodriguez, L.A., Ellis, R.J., Richie, C.T., Harvey, B.K., Dannals, R.F*., et al.* (2017). Chemogenetics revealed: DREADD occupancy and activation via converted clozapine. Science *357*, 503-507.

Gomis, A., Soriano, S., Belmonte, C., and Viana, F. (2008). Hypoosmotic- and pressure-induced membrane stretch activate TRPC5 channels. The Journal of physiology *586*, 5633-5649.

Ha, G.E., Lee, J., Kwak, H., Song, K., Kwon, J., Jung, S.Y., Hong, J., Chang, G.E., Hwang, E.M., Shin, H.S*., et al.* (2016). The Ca(2+)-activated chloride channel anoctamin-2 mediates spike-frequency adaptation and regulates sensory transmission in thalamocortical neurons. Nature communications *7*, 13791.

Hall, J.E., and Guyton, A.C. (2011). Guyton and Hall textbook of medical physiology (Philadelphia: Elsevier Saunders).

Harris, J.A. (1998). Using c-fos as a neural marker of pain. Brain research bulletin *45*, 1-8.
Herbst, K.J., Allen, M.D., and Zhang, J. (2009). The cAMP-dependent protein kinase inhibitor H-89 attenuates the bioluminescence signal produced by Renilla Luciferase. PloS one *4*, e5642.

Heusser, K., Tank, J., Luft, F.C., and Jordan, J. (2005). Baroreflex failure. Hypertension *45*, 834-839.

Holzer, P. (2015). Acid-sensing ion channels in gastrointestinal function. Neuropharmacology *94*, 72-79.

Hong, G.S., Lee, B., Wee, J., Chun, H., Kim, H., Jung, J., Cha, J.Y., Riew, T.R., Kim, G.H., Kim, I.B.*, et al.* (2016). Tentonin 3/TMEM150c Confers Distinct Mechanosensitive Currents in Dorsal-Root Ganglion Neurons with Proprioceptive Function. Neuron *91*, 107-118.

Huang, F., Wang, X., Ostertag, E.M., Nuwal, T., Huang, B., Jan, Y.N., Basbaum, A.I., and Jan, L.Y. (2013). TMEM16C facilitates Na(+)-activated K+ currents in rat sensory neurons and regulates pain processing. Nat Neurosci *16*, 1284-1290.

Huang, F., Zhang, H., Wu, M., Yang, H., Kudo, M., Peters, C.J., Woodruff, P.G., Solberg, O.D., Donne, M.L., Huang, X.*, et al.* (2012a). Calcium-activated chloride channel TMEM16A modulates mucin secretion and airway smooth muscle contraction. Proceedings of the National Academy of Sciences of the United States of America *109*, 16354-16359.

Huang, W.C., Xiao, S., Huang, F., Harfe, B.D., Jan, Y.N., and Jan, L.Y. (2012b). Calcium-activated chloride channels (CaCCs) regulate action potential and synaptic response in hippocampal neurons. Neuron *74*, 179-192.

Huang, Z.J., Li, H.C., Cowan, A.A., Liu, S., Zhang, Y.K., and Song, X.J. (2012c). Chronic compression or acute dissociation of dorsal root ganglion induces cAMP-dependent neuronal hyperexcitability through activation of PAR2. Pain *153*, 1426-1437.

Ichinose, M., and Nishiyasu, T. (2012). Arterial baroreflex control of muscle sympathetic nerve activity under orthostatic stress in humans. Frontiers in physiology *3*, 314.

Iliescu, R., Tudorancea, I., and Lohmeier, T.E. (2014). Baroreflex activation: from mechanisms to therapy for cardiovascular disease. Current hypertension reports *16*, 453.

James, M.A., and Potter, J.F. (1999). Orthostatic blood pressure changes and arterial baroreflex sensitivity in elderly subjects. Age Ageing *28*, 522-530.

Jang, Y., and Oh, U. (2014). Anoctamin 1 in secretory epithelia. Cell calcium *55*, 355-361.

Jentsch, T.J., Steinmeyer, K., and Schwarz, G. (1990). Primary structure of Torpedo marmorata chloride channel isolated by expression cloning in Xenopus oocytes. Nature *348*, 510-514.

Jin, X., Shah, S., Du, X., Zhang, H., and Gamper, N. (2016). Activation of Ca(2+) -activated Cl(-) channel ANO1 by localized Ca(2+) signals. The Journal of physiology *594*, 19-30.

Jun, I., Park, H.S., Piao, H., Han, J.W., An, M.J., Yun, B.G., Zhang, X., Cha, Y.H., Shin, Y.K., Yook, J.I., *et al.* (2017). ANO9/TMEM16J promotes tumourigenesis via EGFR and is a novel therapeutic target for pancreatic cancer. Br J Cancer.

Keckeis, S., Reichhart, N., Roubeix, C., and Strauss, O. (2017a). Anoctamin2 (TMEM16B) forms the Ca2+-activated Cl- channel in the retinal pigment epithelium. Experimental eye research *154*, 139-150.

Keckeis, S., Wernecke, L., Salchow, D.J., Reichhart, N., and Strauss, O. (2017b). Activation of a Ca(2+)-dependent cation conductance with properties of TRPM2 by reactive oxygen species in lens epithelial cells. Experimental eye research *161*, 61-70.

Kim, H., Kim, H., Lee, J., Lee, B., Kim, H.R., Jung, J., Lee, M.O., and Oh, U. (2018). Anoctamin 9/TMEM16J is a cation channel activated by cAMP/PKA signal. Cell calcium *71*, 75-85.

Kim, K.S., Kim, J., Back, S.K., Im, J.Y., Na, H.S., and Han, P.L. (2007). Markedly attenuated acute and chronic pain responses in mice lacking adenylyl cyclase-5. Genes, brain, and behavior *6*, 120-127.

Klabunde, R.E. (2013). Cardiovascular Physiology Concepts (Hagerstown, USA: Lippincott Williams & Wilkins).

Krauhs, J.M. (1979). Structure of rat aortic baroreceptors and their relationship to connective tissue. J Neurocytol *8*, 401-414.

Kupari, J., Haring, M., Agirre, E., Castelo-Branco, G., and Ernfors, P. (2019). An Atlas of Vagal Sensory Neurons and Their Molecular Specialization. Cell reports *27*, 2508-2523 e2504.
Kuruma, A., and Hartzell, H.C. (1999). Dynamics of calcium regulation of chloride currents in Xenopus oocytes. The American journal of physiology *276*, 161-175.

La, J.H., Feng, B., Kaji, K., Schwartz, E.S., and Gebhart, G.F. (2016). Roles of isolectin B4-binding afferents in colorectal mechanical nociception. Pain *157*, 348-354.

Lau, O.C., Shen, B., Wong, C.O., Tjong, Y.W., Lo, C.Y., Wang, H.C., Huang, Y., Yung, W.H., Chen, Y.C., Fung, M.L., *et al.* (2016). TRPC5 channels participate in pressure-sensing in aortic baroreceptors. Nat Commun *7*, 11947.

Lee, B., Cho, H., Jung, J., Yang, Y.D., Yang, D.J., and Oh, U. (2014). Anoctamin 1 contributes to inflammatory and nerve-injury induced hypersensitivity. Mol Pain *10*, 5.

Lerch, T.F., O'Donnell, J.K., Meyer, N.L., Xie, Q., Taylor, K.A., Stagg, S.M., and Chapman, M.S. (2012). Structure of AAV-DJ, a retargeted gene therapy vector: cryo-electron microscopy at 4.5 A resolution. Structure (London, England : 1993) *20*, 1310-1320.

Lewin, M.R., and Walters, E.T. (1999). Cyclic GMP pathway is critical for inducing long-term sensitization of nociceptive sensory neurons. Nature neuroscience *2*, 18-23.

Li, C., Cai, S., Wang, X., and Jiang, Z. (2015). Identification and characterization of ANO9 in stage II and III colorectal carcinoma. Oncotarget *6*, 29324-29334.

Li, R.C., Lin, C.C., Ren, X., Wu, J.S., Molday, L.L., Molday, R.S., and Yau, K.W. (2018). Ca(2+)-activated Cl current predominates in threshold response of mouse olfactory receptor neurons. Proceedings of the National Academy of Sciences of the United States of America *115*, 5570-5575.

Li, Z.H., Cui, D., Qiu, C.J., and Song, X.J. (2019). Cyclic nucleotide signaling in sensory neuron hyperexcitability and chronic pain after nerve injury. Neurobiology of pain (Cambridge, Mass) *6*, 100028.

Loukin, S., Zhou, X., Su, Z., Saimi, Y., and Kung, C. (2010). Wild-type and brachyolmia-causing mutant TRPV4 channels respond directly to stretch force. The Journal of biological chemistry *285*, 27176-27181.

Low, P.A., and Tomalia, V.A. (2015). Orthostatic Hypotension: Mechanisms, Causes, Management. Journal of clinical neurology (Seoul, Korea) *11*, 220-226.

Lu, Y., Ma, X., Sabharwal, R., Snitsarev, V., Morgan, D., Rahmouni, K., Drummond, H.A., Whiteis, C.A., Costa, V., Price, M.*, et al.* (2009). The ion channel ASIC2 is required for baroreceptor and autonomic control of the circulation. Neuron *64*, 885-897.

Lv, M., You, G., Wang, J., Fu, Q., Gupta, A., Li, J., and Sun, J. (2019). Identification of a novel ANO5 missense mutation in a Chinese family with familial florid osseous dysplasia. Journal of human genetics *64*, 599-607.

Mailhot-Larouche, S., Deschenes, L., Lortie, K., Gazzola, M., Marsolais, D., Brunet, D., Robichaud, A., and Bosse, Y. (2018). Assessment of Respiratory Function in Conscious Mice by Double-chamber Plethysmography. Journal of visualized experiments : JoVE.

Malmberg, A.B., Brandon, E.P., Idzerda, R.L., Liu, H., McKnight, G.S., and Basbaum, A.I. (1997). Diminished inflammation and nociceptive pain with preservation of neuropathic pain in mice with a targeted mutation of the type I regulatory subunit of cAMP-dependent protein kinase. The Journal of neuroscience : the official journal of the Society for Neuroscience *17*, 7462-7470.

Malmberg, A.B., and Yaksh, T.L. (1992). Antinociceptive actions of spinal nonsteroidal anti-inflammatory agents on the formalin test in the rat. The Journal of pharmacology and experimental therapeutics *263*, 136-146.

Malysz, J., Gibbons, S.J., Saravanaperumal, S.A., Du, P., Eisenman, S.T., Cao, C., Oh, U., Saur, D., Klein, S., Ordog, T.*, et al.* (2017). Conditional genetic deletion of Ano1 in interstitial cells of Cajal impairs Ca(2+) transients and slow waves in adult mouse small intestine. American journal of physiology Gastrointestinal and liver physiology *312*, G228-g245.

Marconi, C., Brunamonti Binello, P., Badiali, G., Caci, E., Cusano, R., Garibaldi, J., Pippucci, T., Merlini, A., Marchetti, C., Rhoden, K.J.*, et al.* (2012). A novel missense mutation in ANO5/TMEM16E is causative for gnathodiaphyseal dyplasia in a large Italian pedigree. European journal of human genetics : EJHG.

Martinka, P., Fielitz, J., Patzak, A., Regitz-Zagrosek, V., Persson, P.B., and Stauss, H.M. (2005). Mechanisms of blood pressure variability-induced cardiac hypertrophy and

dysfunction in mice with impaired baroreflex. American journal of physiology Regulatory, integrative and comparative physiology *288*, R767-776.

Mostarda, C., Moraes-Silva, I.C., Moreira, E.D., Medeiros, A., Piratello, A.C., Consolim-Colombo, F.M., Caldini, E.G., Brum, P.C., Krieger, E.M., and Irigoyen, M.C. (2011). Baroreflex sensitivity impairment is associated with cardiac diastolic dysfunction in rats. J Card Fail *17*, 519-525.

Nanetti, L., Sarto, E., Castaldo, A., Magri, S., Mongelli, A., Rossi Sebastiano, D., Canafoglia, L., Grisoli, M., Malaguti, C., Rivieri, F*., et al.* (2019). ANO10 mutational screening in recessive ataxia: genetic findings and refinement of the clinical phenotype. Journal of neurology *266*, 378-385.

Nixon, R.A., and Shea, T.B. (1992). Dynamics of neuronal intermediate filaments: a developmental perspective. Cell Motil Cytoskeleton *22*, 81-91.

Nonomura, K., Woo, S.H., Chang, R.B., Gillich, A., Qiu, Z., Francisco, A.G., Ranade, S.S., Liberles, S.D., and Patapoutian, A. (2017). Piezo2 senses airway stretch and mediates lung inflation-induced apnoea. Nature *541*, 176-181.

Norcliffe-Kaufmann, L., Axelrod, F., and Kaufmann, H. (2010). Afferent baroreflex failure in familial dysautonomia. Neurology *75*, 1904-1911.

Numata, T., Shimizu, T., and Okada, Y. (2007). TRPM7 is a stretch- and swelling-activated cation channel involved in volume regulation in human epithelial cells. American journal of physiology Cell physiology *292*, C460-467.

Oh, S.J., Hwang, S.J., Jung, J., Yu, K., Kim, J., Choi, J.Y., Hartzell, H.C., Roh, E.J., and Lee, C.J. (2013). MONNA, a potent and selective blocker for transmembrane protein with unknown function 16/anoctamin-1. Molecular pharmacology *84*, 726-735.

Oh, U., and Jung, J. (2016). Cellular functions of TMEM16/anoctamin. Pflugers Archiv : European journal of physiology *468*, 443-453.

Parkin, M.L., Lim, K., Burke, S.L., and Head, G.A. (2016). Comparison in Conscious Rabbits of the Baroreceptor-Heart Rate Reflex Effects of Chronic Treatment with Rilmenidine, Moxonidine, and Clonidine. Frontiers in physiology *7*, 522.

Parpaite, T., and Coste, B. (2017). Piezo channels. Current biology : CB *27*, R250-r252.

Pedemonte, N., and Galietta, L.J. (2014). Structure and function of TMEM16 proteins (anoctamins). Physiol Rev *94*, 419-459.

Peters, J.H., McDougall, S.J., Fawley, J.A., Smith, S.M., and Andresen, M.C. (2010). Primary afferent activation of thermosensitive TRPV1 triggers asynchronous glutamate release at central neurons. Neuron *65*, 657-669.

Rasche, S., Toetter, B., Adler, J., Tschapek, A., Doerner, J.F., Kurtenbach, S., Hatt, H., Meyer, H., Warscheid, B., and Neuhaus, E.M. (2010). Tmem16b is specifically expressed in the cilia of olfactory sensory neurons. Chem Senses *35*, 239-245.

Riley, T.L., and Friedman, J.M. (1981). Stroke, orthostatic hypotension, and focal seizures. JAMA *245*, 1243-1244.

Rodwell, V.W., Bender, D.A., Botham, K.M., Kennelly, P.J., Weil, P.A., and Harper, H.A. (2018). Harper's illustrated biochemistry.

Sato, T., Kawada, T., Miyano, H., Shishido, T., Inagaki, M., Yoshimura, R., Tatewaki, T., Sugimachi, M., Alexander, J., Jr., and Sunagawa, K. (1999). New simple methods for isolating baroreceptor regions of carotid sinus and aortic depressor nerves in rats. The American journal of physiology *276*, H326-332.

Schmidt, R.M., Kumada, M., and Sagawa, K. (1972). Cardiovascular responses to various pulsatile pressures in the carotid sinus. The American journal of physiology *223*, 1-7.

Schroeder, B.C., Cheng, T., Jan, Y.N., and .Jan, L.Y. (2008). Expression cloning of TMEM16A as a calcium-activated chloride channel subunit. Cell *134*, 1019-1029.

Seagard, J.L., van Brederode, J.F., Dean, C., Hopp, F.A., Gallenberg, L.A., and Kampine, J.P. (1990). Firing characteristics of single-fiber carotid sinus baroreceptors. Circulation research *66*, 1499-1509.

Serezani, C.H., Ballinger, M.N., Aronoff, D.M., and Peters-Golden, M. (2008). Cyclic AMP: master regulator of innate immune cell function. American journal of respiratory cell and molecular biology *39*, 127-132.

Silva, A.M.S., Coimbra-Neto, A.R., Souza, P.V.S., Winckler, P.B., Goncalves, M.V.M., Cavalcanti, E.B.U., Carvalho, A., Sobreira, C., Camelo, C.G., Mendonca, R.D.H.*, et al.* (2019). Clinical and molecular findings in a cohort of ANO5-related myopathy. Annals of clinical and translational neurology *6*, 1225-1238.

Simonetti, M., Agarwal, N., Stosser, S., Bali, K.K., Karaulanov, E., Kamble, R., Pospisilova, B., Kurejova, M., Birchmeier, W., Niehrs, C.*, et al.* (2014). Wnt-Fzd signaling sensitizes peripheral sensory neurons via distinct noncanonical pathways. Neuron *83*, 104-121.

Song, X., Gao, X., Guo, D., Yu, Q., Guo, W., He, C., Burnstock, G., and Xiang, Z. (2012). Expression of P2X(2) and P2X (3) receptors in the rat carotid sinus, aortic arch, vena cava, and heart, as well as petrosal and nodose ganglia. Purinergic Signal *8*, 15-22.

Song, X.J., Wang, Z.B., Gan, Q., and Walters, E.T. (2006). cAMP and cGMP contribute to sensory neuron hyperexcitability and hyperalgesia in rats with dorsal root ganglia compression. Journal of neurophysiology *95*, 479-492.

Stanich, J.E., Gibbons, S.J., Eisenman, S.T., Bardsley, M.R., Rock, J.R., Harfe, B.D., Ordog, T., and Farrugia, G. (2011). Ano1 as a regulator of proliferation. American journal of physiology Gastrointestinal and liver physiology *301*, G1044-1051.

Stork, P.J., and Schmitt, J.M. (2002). Crosstalk between cAMP and MAP kinase signaling in the regulation of cell proliferation. Trends in cell biology *12*, 258-266.

Strickland, M., Yacoubi-Loueslati, B., Bouhaouala-Zahar, B., Pender, S.L.F., and Larbi, A.

(2019). Relationships Between Ion Channels, Mitochondrial Functions and Inflammation in Human Aging. Frontiers in physiology *10*, 158.

Sun, H., Li, D.P., Chen, S.R., Hittelman, W.N., and Pan, H.L. (2009). Sensing of blood pressure increase by transient receptor potential vanilloid 1 receptors on baroreceptors. The Journal of pharmacology and experimental therapeutics *331*, 851-859.

Susaki, E.A., Tainaka, K., Perrin, D., Kishino, F., Tawara, T., Watanabe, T.M., Yokoyama, C., Onoe, H., Eguchi, M., Yamaguchi, S.*, et al.* (2014). Whole-brain imaging with single-cell resolution using chemical cocktails and computational analysis. Cell *157*, 726-739.

Susaki, E.A., Tainaka, K., Perrin, D., Yukinaga, H., Kuno, A., and Ueda, H.R. (2015). Advanced CUBIC protocols for whole-brain and whole-body clearing and imaging. Nat Protoc *10*, 1709-1727.

Suzuki, J., Umeda, M., Sims, P., and Nagata, S. (2010). Calcium dependent phospholipid scrambling by TMEM16F. Nature *468*, 834–838.

Sykora, M., Diedler, J., Poli, S., Rupp, A., Turcani, P., and Steiner, T. (2010). Blood pressure course in acute stroke relates to baroreflex dysfunction. Cerebrovasc Dis *30*, 172-179.

Szczot, M., Liljencrantz, J., Ghitani, N., Barik, A., Lam, R., Thompson, J.H., Bharucha-Goebel, D., Saade, D., Necaise, A., Donkervoort, S.*, et al.* (2018). PIEZO2 mediates injury-induced tactile pain in mice and humans. Science translational medicine *10*.

Taiwo, Y.O., Bjerknes, L.K., Goetzl, E.J., and Levine, J.D. (1989). Mediation of primary afferent peripheral hyperalgesia by the cAMP second messenger system. Neuroscience *32*, 577-580.

Thrasher, T.N. (2005). Baroreceptors, baroreceptor unloading, and the long-term control of blood pressure. American journal of physiology Regulatory, integrative and comparative physiology *288*, R819-827.

Tominaga, M., Caterina, M.J., Malmberg, A.B., Rosen, T.A., Gilbert, H., Skinner, K., Raumann, B.E., Basbaum, A.I., and Julius, D. (1998). The cloned capsaicin receptor integrates multiple pain-producing stimuli. Neuron *21*, 531-543.

Vasquez, E.C., Meyrelles, S.S., Mauad, H., and Cabral, A.M. (1997). Neural reflex regulation of arterial pressure in pathophysiological conditions: interplay among the baroreflex, the cardiopulmonary reflexes and the chemoreflex. Brazilian journal of medical and biological research = Revista brasileira de pesquisas medicas e biologicas *30*, 521-532.

Victor, R.G. (2015). Carotid baroreflex activation therapy for resistant hypertension. Nat Rev Cardiol *12*, 451-463.

Voss, A., Malberg, H., Schumann, A., Wessel, N., Walther, T., Stepan, H., and Faber, R. (2000). Baroreflex sensitivity, heart rate, and blood pressure variability in normal pregnancy. Am J Hypertens *13*, 1218-1225.

Wang, J., Kollarik, M., Ru, F., Sun, H., McNeil, B., Dong, X., Stephens, G., Korolevich, S.,

Brohawn, P., Kolbeck, R.*, et al.* (2017). Distinct and common expression of receptors for inflammatory mediators in vagal nodose versus jugular capsaicin-sensitive/TRPV1-positive neurons detected by low input RNA sequencing. PloS one *12*, e0185985.

Wang, L., Zhou, H., Zhang, M., Liu, W., Deng, T., Zhao, Q., Li, Y., Lei, J., Li, X., and Xiao, B. (2019). Structure and mechanogating of the mammalian tactile channel PIEZO2. Nature *573*, 225-229.

Wang, Q., Leo, M.D., Narayanan, D., Kuruvilla, K.P., and Jaggar, J.H. (2016). Local coupling of TRPC6 to ANO1/TMEM16A channels in smooth muscle cells amplifies vasoconstriction in cerebral arteries. American journal of physiology Cell physiology *310*, C1001-1009.

Wess, J., Nakajima, K., and Jain, S. (2013). Novel designer receptors to probe GPCR signaling and physiology. Trends Pharmacol Sci *34*, 385-392.

West, R.B., Corless, C.L., Chen, X., Rubin, B.P., Subramanian, S., Montgomery, K., Zhu, S., Ball, C.A., Nielsen, T.O., Patel, R.*, et al.* (2004). The novel marker, DOG1, is expressed ubiquitously in gastrointestinal stromal tumors irrespective of KIT or PDGFRA mutation status. The American journal of pathology *165*, 107-113.

Wilkinson, K.D., Lee, K.M., Deshpande, S., Duerksen-Hughes, P., Boss, J.M., and Pohl, J. (1989). The neuron-specific protein PGP 9.5 is a ubiquitin carboxyl-terminal hydrolase. Science *246*, 670-673.

Wine, J.J., Brayden, D.J., Hagiwara, G., Krouse, M.E., Law, T.C., Muller, U.J., Solc, C.K., Ward, C.L., Widdicombe, J.H., and Xia, Y. (1991). Cystic fibrosis, the CFTR, and rectifying Cl- channels. Advances in experimental medicine and biology *290*, 253-269; discussion 269-272.

Woo, S.H., Lukacs, V., de Nooij, J.C., Zaytseva, D., Criddle, C.R., Francisco, A., Jessell, T.M., Wilkinson, K.A., and Patapoutian, A. (2015). Piezo2 is the principal mechanotransduction channel for proprioception. Nature neuroscience *18*, 1756-1762.

Worrell, R.T., Butt, A.G., Cliff, W.H., and Frizzell, R.A. (1989). A volume-sensitive chloride conductance in human colonic cell line T84. The American journal of physiology *256*, C1111-1119.

Xu, Z., Lefevre, G.M., Gavrilova, O., Foster St Claire, M.B., Riddick, G., and Felsenfeld, G. (2014). Mapping of long-range INS promoter interactions reveals a role for calcium-activated chloride channel ANO1 in insulin secretion. Proceedings of the National Academy of Sciences of the United States of America *111*, 16760-16765.

Yam, M.F., Loh, Y.C., Tan, C.S., Khadijah Adam, S., Abdul Manan, N., and Basir, R. (2018). General Pathways of Pain Sensation and the Major Neurotransmitters Involved in Pain Regulation. International journal of molecular sciences *19*.

Yamamizu, K., and Yamashita, J.K. (2011). Roles of cyclic adenosine monophosphate signaling in endothelial cell differentiation and arterial-venous specification during vascular development. Circulation journal : official journal of the Japanese Circulation Society *75*, 253-260.

Yang, H., Kim, A., David, T., Palmer, D., Jin, T., Tien, J., Huang, F., Cheng, T., Coughlin, S.R., Jan, Y.N., *et al.* (2012). TMEM16F forms a Ca2+-activated cation channel required for lipid scrambling in platelets during blood coagulation. Cell *151*, 111-122.

Yang, Y.D., Cho, H., Koo, J., Tak, M.H., Cho, Y., Shim, W.S., Park, S.P., Lee, J., Lee, B., Kim, B.M., *et al.* (2008a). TMEM16A confers receptor-activated calcium-dependent chloride conductance. Nature *455*, 1210-1215.

Yang, Y.D., Cho, H., Koo, J.Y., Tak, M.H., Cho, Y., Shim, W.S., Park, S.P., Lee, J., Lee, B., Kim, B.M., *et al.* (2008b). TMEM16A confers receptor-activated calcium-dependent chloride conductance. Nature *455*, 1210-1215.

Yin, D., and Slavin, K.V. (2015). Carotid Sinus/Nerve Stimulation for Treatment of Resistant Hypertension and Heart Failure. Prog Neurol Surg *29*, 83-93.

Yu, K., Whitlock, J.M., Lee, K., Ortlund, E.A., Cui, Y.Y., and Hartzell, H.C. (2015). Identification of a lipid scrambling domain in ANO6/TMEM16F. eLife *4*, e06901.
Yu, K., Zhu, J., Qu, Z., Cui, Y.Y., and Hartzell, H.C. (2014). Activation of the Ano1 (TMEM16A) chloride channel by calcium is not mediated by calmodulin. The Journal of general physiology *143*, 253-267.

Zeng, W.Z., Marshall, K.L., Min, S., Daou, I., Chapleau, M.W., Abboud, F.M., Liberles, S.D., and Patapoutian, A. (2018). PIEZOs mediate neuronal sensing of blood pressure and the baroreceptor reflex. Science *362*, 464-467.

Zhang, Y., Zhang, Z., Xiao, S., Tien, J., Le, S., Le, T., Jan, L.Y., and Yang, H. (2017). Inferior Olivary TMEM16B Mediates Cerebellar Motor Learning. Neuron *95*, 1103-1111.e1104.
Zheng, J. (2013). Molecular mechanism of TRP channels. Comprehensive Physiology *3*, 221-242.

Zhu, G., Dong, Y., He, X., Zhao, P., Yang, A., Zhou, R., Ma, J., Xie, Z., and Song, X.J. (2016). Radiotherapy Suppresses Bone Cancer Pain through Inhibiting Activation of cAMP Signaling in Rat Dorsal Root Ganglion and Spinal Cord. Mediators of inflammation *2016*, 5093095.

국 문 초 록

TTN3으로도 알려진 TMEM150C는 기계적 자극에 의해 활성화 될 수 있는 양이온 채널이다. TTN3의 비활성화는 Piezo1 또는 Piezo2가 빠르게 비활성화 되는 것과 비교하여 느리게 일어난다. TTN3이 근육방추의 구심성 신경에서 발현되고 근육 운동을 조절하는 것으로 이전에 보고 된 바 있다. 그 이후, 본 저자는 TTN3이 Baroreceptor 구심성섬유 (Nodose ganglia, NG)의 신경세포에서 현저하게 발현되는 것을 발견했다. TTN3은 기계적 감각에 의해 반응하는 채널이기 때문에, TTN3이 압력수용기가 혈압 변화를 감지하는 데 관여 할 수 있다는 가설을 세우고 실험하였다. 이 논문에서 TTN3가 대동맥 궁과 구심성섬유 뉴런의 신경 말단에서 발현되는 것을 확인하였다. Ttn3 KO 쥐에서 말초 고혈압, 빈맥, 혈압의 큰 변동 등이 일어나고, 압력 수용기의 기능이 망가진 것을 확인되었다. Chemogenetic을 이용하여 Ttn3가 발현된 NG의 뉴런을 억제 혹은 자극 시킬 때, 혈압 및 심박수가 증가 혹은 감소되는 것을 확인하였다. 또, Ttn3 KO 쥐의 NG에서 Ttn3를 다시 재발현시킨 경우, KO에서 일어났던 심혈관 변화가 회복되었다. 이러한 결과로 미루어 볼 때, 본 논문은 TTN3이 압력수용체에서 혈압의 동적 변화를 감지하는 데 중요하게 기여한다고 보고한다.

아녹타민 (ANO) 유전자 패밀리로도 알려진 TMEM16은 10개의 이성체로 구성된다. ANO1 및 ANO2는 Ca2+ 에 의해 활성화 되는 음이온 채널이다. ANO6는 막에서 분극된 인지질을 파괴하는 지질 파괴 효소로 알려졌다. 그러

나 아직까지 TMEM16H (ANO8)의 기능에 대해서는 알려지지 않았다. 이 논문에서 본 저자는 ANO8/TMEM16H가 세포 내 cAMP에 의해 활성화 된 양이온 채널이라는 것을 발견했다. 세포 내 cAMP에 의해 ANO8가 과발현 된 HEK 세포에서 전류가 유발되었다. cAMP-의존적 전류는 Protein kinase A 억제제에 의해 억제되는데, 이는 PKA가 ANO8을 활성화 시킨다는 것을 보여준다. Adenylyl cyclase를 활성화시키는 콜레라 독소도 ANO8을 활성화 시켰다. cAMP에 의해 유도 된 ANO8 발현 세포의 전류는 양이온이었고, 이는 선택적으로 특정 양이온을 투과시키지는 않았다. ANO8은 뇌에서의 뉴런 및 배근 신경절 (DRG) 뉴런에서 고도로 발현되어 있다. Ano8의 knockdown을 시킨 경우, 포르말린 통증 마우스 모델에서 통각이 감소되고, DRG 뉴런에서 cAMP- 의존적 전류의 감소도 일어났다. 이러한 결과는 ANO8이 cAMP 경로에 의해 활성화되고 통증 경로에서의 통각에 관여하는 양이온 채널 임을 시사한다.

학 번: 2015-30875

주요어 : TMEM150C / TTN3, TMEM16H / ANO8, 이온 채널, Baroreceptor, 통각, cAMP / PKA, 통증